

Utah State University

DigitalCommons@USU

All Graduate Theses and Dissertations, Spring
1920 to Summer 2023

Graduate Studies

8-2023

Laboratory Measurements at the Impact Point of a Falling Jet

Garrett Richins
Utah State University

Follow this and additional works at: <https://digitalcommons.usu.edu/etd>



Part of the [Civil and Environmental Engineering Commons](#)

Recommended Citation

Richins, Garrett, "Laboratory Measurements at the Impact Point of a Falling Jet" (2023). *All Graduate Theses and Dissertations, Spring 1920 to Summer 2023*. 8890.
<https://digitalcommons.usu.edu/etd/8890>

This Thesis is brought to you for free and open access by the Graduate Studies at DigitalCommons@USU. It has been accepted for inclusion in All Graduate Theses and Dissertations, Spring 1920 to Summer 2023 by an authorized administrator of DigitalCommons@USU. For more information, please contact digitalcommons@usu.edu.



LABORATORY MEASUREMENTS AT THE IMPACT POINT OF A FALLING JET

by

Garrett Richins

A thesis submitted in partial fulfillment
of the requirements for the degree

of

MASTER OF SCIENCE

in

Civil and Environmental Engineering

Approved:

Steven L. Barfuss, M.S.
Major Professor

Zachary B. Sharp, Ph.D.
Committee Member

Michael C. Johnson, Ph.D.
Committee Member

John D. Rice, Ph.D.
Committee Member

D. Richard Cutler, Ph.D.
Vice Provost of Graduate Studies

UTAH STATE UNIVERSITY
Logan, Utah

2023

Copyright © Garrett Richins 2023

All Rights Reserved

ABSTRACT

Laboratory Measurements at the Impact Point of a Falling Jet

by

Garrett Richins, Master of Science

Utah State University, 2023

Major Professor: Steven L. Barfuss
Department: Civil and Environmental Engineering

Physical testing of scale models is an important aspect in the design and evaluation of hydraulic structures. A falling jet is a component of such physical testing. The focus of concern at the terminus of the jet is potential scour. Subsequently, during physical model studies it is necessary to record the pressure at the terminus. Several methods are used to monitor or evaluate this pressure. Different results from the different methods have been observed in a laboratory setting, which has become the focus of this study.

This study was conducted to evaluate the different methods by setting up a physical model of a falling jet and measuring pressure at the point of impact on a flat, horizontal plate using different instrumentation. The instrumentation tested included a flush mounted transducer, a pressure transmitter, and a piezometer. A computational fluid dynamics simulation and calculations using equations of energy and momentum were also completed as another way to estimate the pressure at the impact point of a falling jet.

Testing was conducted at the Utah Water Research Laboratory (UWRL). The jet nozzle had an I.D. of 2.05 inches. The falling water jet was tested at fall heights of 2-, 5-, and 10-feet. Up to

four flow rates were tested at each height at a range of approximately 50-220 gpm. The flush mounted transducer, pressure transmitter, and piezometer produced similar results at the 2-ft and 5-ft fall heights. At the 10-ft fall height, the resulting pressure from the flush mounted transducer was notably different from pressures recorded using the pressure transmitter and the piezometer.

The pressures recorded or calculated using the various methods provides a guide for choosing the instrumentation to use when monitoring pressure at the impact point of a falling jet in a physical model. The data collected will also aid in evaluating the pressure results obtained using a certain method of measurement or calculation. (9515)

(89 pages)

PUBLIC ABSTRACT

Laboratory Measurements at the Impact Point of a Falling Jet

Garrett Richins

Dams and spillways play a vital role in managing water resources. Many of these hydraulic structures feature a falling jet when discharging downstream. Engineers design plunge pools to receive jets with enough water depth or a protective liner to protect the river bottom so that scour is avoided. Quantifying the pressures at the bottom of the falling jet is a key component to determining the potential for scour and the need for mitigation techniques.

In the laboratory setting, significant discrepancies have been observed between different measurement methods to measure mean and fluctuating pressures of a falling jet intercepting a solid physical boundary. The focus of this research was to evaluate measurable discrepancies between different measurement methods at the impact point on a solid boundary of a falling jet. The laboratory measurements of this study were also compared to numerical modeling and theoretical calculation methods.

A laboratory test fixture was constructed to monitor pressures induced by the falling jet using the following instruments: a flush mounted pressure transducer, a pressure transmitter, and a piezometer. Jet velocity and fall height were the variables associated with this testing. The test fixture conditions were also simulated numerically with computational fluid dynamics and calculated using fundamental equations of momentum. These numerical and theoretical calculation methods simply provided another measurement for comparison.

It was the aim of this study to make conclusions about the appropriate use of different methods of measurement in this scenario. Trends were identified that give insight into the pressures resulting from the various measurement methods. The flush mounted transducer, pressure transmitter, and piezometer produced similar results at the 2-ft and 5-ft fall heights. At the 10-ft fall height, the resulting pressure from the flush mounted transducer was notably different from pressures recorded using the pressure transmitter and the piezometer. This paper discusses conclusions that have been made regarding the most acceptable methods for measuring pressure at the impact point of a falling jet in a laboratory setting.

ACKNOWLEDGMENTS

The help of several individuals made this work possible. My major professor, Steve Barfuss, gave guidance throughout the process of choosing a research topic, developing a test plan, analyzing and understanding the data, and writing. Ken Provard, research engineer at the Utah Water Research Laboratory (UWRL), worked many hours constructing the laboratory test setup. Zac Sharp, shop manager at the UWRL, pointed out several factors to consider during research and testing in a laboratory setting and directed the CFD simulation. Jake Douglas completed the CFD simulation. Mike Johnson, UWRL faculty, provided insight on best practices when setting up the laboratory testing. Reilly Hendrix and Matthew Fugal, research assistants, helped with aspects of the laboratory test setup and testing itself. John Rice, Civil and Environmental Engineering faculty at Utah State University, gave feedback on the written report. All members of the committee also gave their thoughts and comments on the written report. Other shop workers at the UWRL provided support and guidance during testing.

I could not have done this without the help and encouragement of my wife, Kennadee, and the inspiration of my two sons, Weston and McKade.

Garrett Richins

CONTENTS

	Page
ABSTRACT.....	iii
PUBLIC ABSTRACT	v
ACKNOWLEDGMENTS	vii
LIST OF TABLES.....	ix
LIST OF FIGURES.....	x
LIST OF NOTATIONS AND SYMBOLS.....	xiii
INTRODUCTION.....	1
BACKGROUND.....	2
PROCEDURE.....	4
Laboratory Tests	4
Calculated Impact Force	11
Computational Fluid Dynamics Simulations	13
RESULTS.....	14
Laboratory Tests	14
Calculated Impact Force	23
Computational Fluid Dynamics Simulations	24
Results Summary	30
DISCUSSION.....	32
Laboratory Tests at a 10-ft fall Height.....	33
Laboratory Tests at a 5-ft fall Height.....	34
Laboratory Tests at a 2-ft fall Height.....	35
Other Observations for Laboratory Tests.....	35
Comparison to Previous Study.....	41
Calculated Impact Force	43
Computational Fluid Dynamics Simulation.....	45
Repeat Tests.....	45
Potential Sources of Error in Laboratory Tests.....	46
Other Variables	46
CONCLUSIONS.....	47
REFERENCES.....	51
APPENDICES.....	52

Appendix A - CALIBRATION OF MAGNETIC FLOW METER.....	53
Appendix B - DRAWINGS OF LABORATORY TEST SETUP	54
Appendix C - TABULAR PRESSURES UNDER A FALLING JET	55
Appendix D - LABORATORY TESTING PHOTOGRAPHS.....	59

LIST OF TABLES

	Page
Table 1. CFD simulation data collection frequency.	13
Table 2. Mean pressure (psi) from laboratory tests and CFD at 4.76 fps and 2-ft fall height.....	45
Table A-1. Utah Water Research Laboratory flow meter calibration data for 6-inch meter.	53
Table C-1. Pressure recorded under jet for the 1 st run at a 2-foot fall height.....	55
Table C-2. Pressure recorded under jet for the 1 st run at a 5-foot fall height.....	55
Table C-3. Pressure recorded under jet for the 1 st run at a 10-foot fall height.....	56
Table C-4. Pressure recorded under jet for the 2 nd run at a 2-foot fall height.....	56
Table C-5. Pressure recorded under jet for the 2 nd run at a 5-foot fall height.....	57
Table C-6. Pressure recorded under jet for the 2 nd run at a 10-foot fall height.....	57
Table C-7. Pressure recorded under jet for the 3 rd run at a 2-foot fall height.	58
Table C-8. Pressure recorded under jet for the 3 rd run at a 5-foot fall height.	58
Table C-9. Pressure recorded under jet for the 3 rd run at a 10-foot fall height.	58

LIST OF FIGURES

	Page
Figure 1. Water line to supply falling jet nozzle (flow goes top to bottom).....	5
Figure 2. Vertical section of the water supply line.	6
Figure 3. 2-inch diameter, steel pipe nipple.....	7
Figure 4. Plexiglass platform for testing instrumentation.....	8
Figure 5. Impact pressure head for various flowrates at a fall height of 2 feet.....	15
Figure 6. Impact pressure head for various flowrates at a fall height of 5 feet.....	16
Figure 7. Impact pressure head for various flowrates at a fall height of 10 feet.....	17
Figure 8. Impact pressure head for various flowrates using a flush mounted transducer.	18
Figure 9. Impact pressure head for various flowrates using a pressure transmitter.....	19
Figure 10. Impact pressure head for various flowrates using a piezometer.....	20
Figure 11. Jet diameter at impact for various flowrates and fall heights.	21
Figure 12. Percent air content at impact for various flowrates and fall heights.....	22
Figure 13. Impact force calculated with equations of momentum.....	23
Figure 14. Laboratory test pressure using pressure transmitter for 2-ft fall height.....	24
Figure 15. CFD pressure data plotted over time for 2-ft fall height.	25
Figure 16. Sample of CFD and physical test data at 2-ft fall height.....	25
Figure 17. Laboratory test pressure data using pressure transmitter for 5-ft fall height.	26
Figure 18. CFD pressure data plotted over time for 5-ft fall height.	26
Figure 19. Sample of CFD and physical test data at 5-ft fall height.....	27
Figure 20. Laboratory test pressure data using pressure transmitter for 10-ft fall height.	27
Figure 21. CFD pressure data plotted over time for 10-ft fall height.	28
Figure 22. Sample of CFD & physical test data at 10-ft fall height.....	28
Figure 23. Force on solid, impact boundary from CFD model.....	29
Figure 24. Pressure data from various sources for a 2-ft fall height.....	30

Figure 25. Pressure data from various sources for a 5-ft fall height.....	31
Figure 26. Pressure data from various sources for a 10-ft fall height.....	32
Figure 27. Impact pressure head at a fall height of 10 feet (with annotations).....	34
Figure 28. Range of pressures for 2-foot fall height.....	36
Figure 29. Range of pressures for 5-foot fall height.....	37
Figure 30. Range of pressures for 10-foot fall height.....	38
Figure 31. Jet diameter at impact with annotations	39
Figure 32. Air content of jet with annotations.....	40
Figure 33. Fall duration of jet for different fall heights & flow rates.....	41
Figure 34. Impact pressure at 2-foot fall height for this study and Fathi et al.....	42
Figure 35. Force on test platform in CFD model and calculations plotted against fall height.	44
Figure B-1. Plan view of laboratory testing setup.....	54
Figure B-2. Side view of vertical section of laboratory test setup.....	54
Figure D-1. Falling jet at approximately 5 fps and 2-foot fall height.....	59
Figure D-2. Falling jet approximately 14 fps and 2-foot fall height.....	60
Figure D-3. Falling jet approximately 19 fps and 2-foot fall height.....	61
Figure D-4. Falling jet approximately 22 fps and 2-foot fall height.....	62
Figure D-5. Falling jet at approximately 5 fps and 5-foot fall height.....	63
Figure D-6. Falling jet at approximately 14 fps and 5-foot fall height.....	64
Figure D-7. Falling jet at approximately 19 fps and 5-foot fall height.....	65
Figure D-8. Falling jet at approximately 22 fps and 5-foot fall height.....	66
Figure D-9. Falling jet at approximately 5 fps and 10-foot fall height (upper section).....	67
Figure D-10. Falling jet at approximately 5 fps and 10-foot fall height (lower section).....	68
Figure D-11. Falling jet at approximately 14 fps and 10-foot fall height (upper section).....	69
Figure D-12. Falling jet at approximately 14 fps and 10-foot fall height (lower section).....	70
Figure D-13. Falling jet at approximately 19 fps and 10-foot fall height (upper section).....	71

Figure D-14. Falling jet at approximately 19 fps and 10-foot fall height (lower section). 72

Figure D-15. Falling jet at approximately 22 fps and 10-foot fall height (upper section). 73

Figure D-16. Falling jet at approximately 22 fps and 10-foot fall height (lower section). 74

LIST OF NOTATIONS AND SYMBOLS

$^{\circ}\text{F}$ – degrees Fahrenheit

θ – angle of impact to solid, physical boundary

A – cross-sectional area of jet

CFD – computational fluid dynamics

cm – centimeters

ft – feet

FT – flush mounted transducer

F – force orthogonal to the solid, physical boundary

g – acceleration due to gravity

gpm – gallons per minute

H – fall height of jet

Hz – Hertz

inHg – inches of Mercury

kHz – kilohertz

m – meters

NIST – National Institute of Standards and Technology

ρ – density of water

P – piezometer

psi – pounds per square inch

psia – pounds per square inch absolute

psig – pound per square inch gauge

PVC – polyvinyl chloride

Q – flow rate of the jet

T – pressure transmitter

V – volts

v – jet velocity

v_i – jet velocity at the impact point on a solid boundary

v_o – initial jet velocity

INTRODUCTION

Dams are an important part of water resource management. They play vital roles in water storage and flood control. When sending water downstream of a dam, spillways are used to control the discharge of large flow rates safely and efficiently. Designing dams and spillways is a complex process requiring expertise from an interdisciplinary group of professionals. Engineers rely on latest research, past projects, and modeling to arrive at an effective design. Modeling can be done physically and numerically. Even with the frequent use of numerical modeling, physical modeling of hydraulic structures continues to provide invaluable insight for engineers. It allows for real-time observation of a scaled version of the structure and it allows engineers to accurately visualize and make decisions about three-dimensional flow patterns, separation zones, and locations of scour potential. Pressure is commonly monitored and analyzed in these models. Some designs of spillways incorporate a falling jet to dissipate energy. A piezometer, pressure transmitter, or transducer may be used in a physical model against a solid boundary to collect pressure data at the point of impact of the falling jet or in the bottom of a scour hole.

Laboratory testing has revealed significant measurable differences in pressure in the same scenario when different instrumentation for measurement is used. It is important to understand the pressure at the point of impact against a solid boundary. Published research and documentation provide insights into the characteristics of a falling jet, calculating pressure under a jet, and laboratory instrumentation used to monitor water pressure.

BACKGROUND

Fathi et al. conducted a study “*to estimate mean core impact pressure of a vertical jet on smooth and rough bar surfaces and weight of the jet Froude number as governing parameters. Relation of turbulence intensity coefficient and the jet breakup length with Froude number is also discussed*” (Fathi-Moghadam et al. 2019). Fathi et al. propose the idea of using a vertically falling jet to dissipate energy at a hydraulic structure, such as a dam, instead of the conventional horizontally discharging jet. He cited a case in Iran where a horizontal jet could damage structures downstream. The jet was discharging into a narrow, winding canyon. To design for this in future scenarios, he assessed the impact of a vertically falling jet on smooth and rough surfaces. The impact was measured in the core of the jet before it was developed. Dynamic pressures in the jet core are higher than in a developed jet. On the other hand, a developed jet has more fluctuations in the dynamic pressures. In his research, connections were made between Froude number and jet core length. A correlation was also made between the jet core length and the turbulence intensity coefficient.

The experiments performed by Fathi et al. are worth attempting to reproduce in the current study. One of the nozzle diameters Fathi et al. used was 5.1 cm. This matched the 2-inch diameter nozzle used in the current study. The fall heights used by Fathi et al. were 8, 15, 25, 35, and 60 cm. The tallest height is almost 2 feet. Piezometer tubes were connected to the impact plate to measure the dynamic pressure. The same tubes were then connected to pressure transmitters (type WIKA, model S-11, sampling rate capability of 10 kHz and accuracy of +/- 0.01 m) to measure instantaneous pressure and fluctuations.

The current study has built upon the work of Fathi et al. It was supposed that the current study would possibly reveal limitations to the equation presented by Fathi et al. The development of the estimation of pressures under a jet is based on impact of the core of a jet. The Fathi et al. equation

was not created to design for pressures in the developed part of a jet. This study has considered possible limitations of instrumentation in measuring the vertically falling jet.

Beltaos et al. (Beltaos and Rajaratnam 1973) studied a turbulent jet impinging a flat surface, normal to the surface. The falling jet was studied analytically and experimentally. The experiment used air for the test fluid. It recorded velocities, pressures, and shear stresses in three different zones of the jet. The zones include the free jet, impinging jet, and wall jet. There was found to be static pressure in the stagnation point of the jet. Jets with differing Reynolds numbers were tested. Different distances between the nozzle and wall were tested. The nozzle was 0.088 inches wide.

Ervine et al. (Ervine et al. 1997) described the different zones of a falling jet. They presented an equation to estimate the boundary of the jet core as it tapers off. They state that surface tension and turbulence affect the distance to the jet breakup point. They stated that identifying the location of the breakup point is important and they found that the jet behaved very differently before and after breakup. After breakup, the impact pressures were found to be lower, but the fluctuations were greater compared to before breakup. An equation for estimating the breakup length of the jet was provided. Flush mounted transducers were used in these tests to measure dynamic pressures at the bottom of the plunge pool.

The study by Ervine et al. ultimately provided practicing engineers with a method for estimating mean and fluctuating pressure fields for falling jets entering plunge pools. Coefficients for mean and fluctuating pressures were found to make this estimate. These two parameters depend on the degree of jet break-up when entering the pool and the aeration of the pool.

PROCEDURE

Laboratory Tests

A testing apparatus was constructed to record pressures from a falling jet at the impact point on a solid boundary. The testing was completed in the Utah Water Research Laboratory at Utah State University in Logan, Utah. Water was supplied from a pipe supply line that was conveyed from the reservoir at First Dam of the Logan River.

The test setup consisted of a supply pipeline and a platform to house the pressure-reading instrumentation. The instrumentation included a flush mounted transducer, a pressure transmitter and a piezometer. The flush mounted transducer was a Keller PR-35X transducer with a pressure span of -0.5 to 0.5 bar and an accuracy of $\pm 0.05\%$. The pressure is in gauge pressure. The pressure transmitter was a Keller 23SX transmitter with a pressure span of 0-40 psia and an accuracy of $\pm 0.1\%$. This transmitter had a 205-inch-long length of water filled $\frac{1}{4}$ -inch O.D. plastic tube connected to the upstream side of it. The pressure was measured in absolute pressure. The piezometer was installed with the use of a $\frac{1}{4}$ -inch O.D. plastic tube that was approximately 198 inches long to the vertical measurement section of the piezometer.

An 8-inch valve was installed 80 feet upstream of the jet nozzle. The supply pipe was reduced to a 6-inch PVC pipe downstream of this valve. After 25 feet of 6-inch PVC pipe, another valve was installed. A 6-inch magnetic flow meter installed in this section of the approach piping was used to measure flowrates throughout testing. The meter was installed 16.5 feet downstream of the 6-inch valve. The flow meter was a 6-inch Siemens SITRANS F M MAGFLO, MAG6000.

Calibration for the meter was completed at the Utah Water Research Laboratory. Calibration

documentation is shown in Table A-1 in Appendix A. The supply line containing the 6-inch magnetic flow meter is shown in Figure 1.

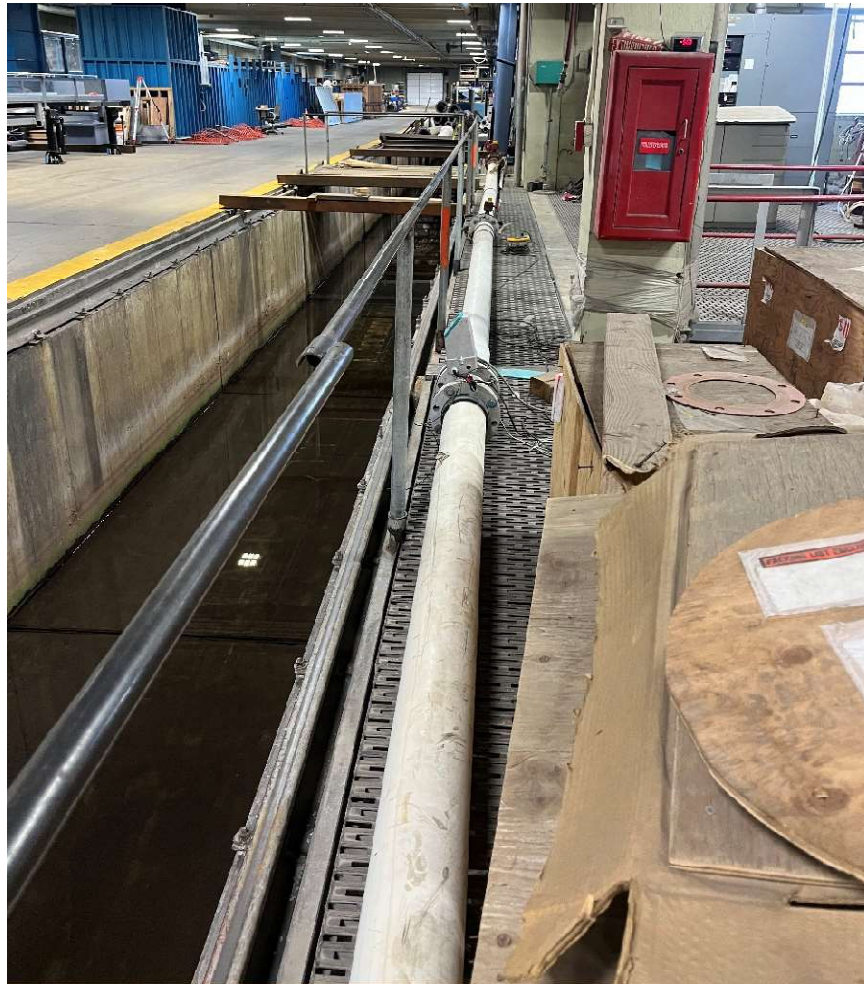


Figure 1 – Water line to supply falling jet nozzle (flow goes top to bottom).

The last several feet of the water line consisted of two vertical bends to direct the nozzle down and orthogonal to the horizontally positioned instrumentation platform. A photograph of this section of the supply line is shown in Figure 2.

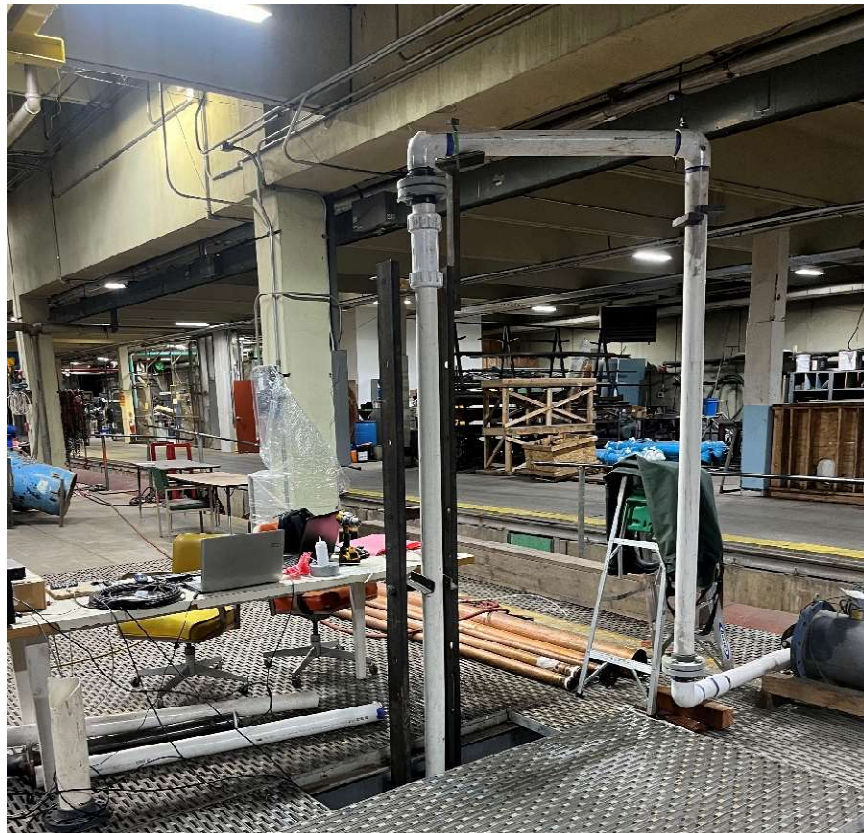


Figure 2 – Vertical section of the water supply line.

The jet nozzle was a steel pipe nipple with an I.D. of 2.05 inches. It was connected to a 3-inch PVC pipe with a steel reducer. Details of the supply line are shown in the drawings shown in

Figures B-1 & B-2 in Appendix B. A photograph of the nozzle used for laboratory tests is shown in Figure 3.



Figure 3 – 2-inch diameter, steel pipe nipple.

A ball valve was located on the top of the pipe between the two vertical bends at the highest point in the supply line. This valve was used to release air. The pressure at this valve would often be lower than atmospheric pressure so it was important to ensure that there were no leaks so that air would not be drawn into the pipe. Before any testing was performed, the flowrate was increased with the ball valve open until the pressure exceeded atmospheric pressure so that all air could be released from the system. The valve was then closed for the remainder of testing.

The configuration of the instrumentation platform allowed for the use of the same platform while testing the three different methods of measuring pressure at the impact point of the jet. Again, the three methods of measuring were a piezometer, flush mounted transducer, and a pressure transmitter. These were each housed in the plexiglass platform shown in Figure 4.



Figure 4 – Plexiglass platform for testing instrumentation.

The platform was carefully leveled and bolted to the floor of a concrete tank that was approximately 10 feet deep. The dimensions of the concrete tank were 18' by 20' with a drain in the middle to drain water that sprayed off the sides of the testing platform.

The transducer and transmitter were wired to StrainSmart, a data logging hardware. Both the piezometer and the pressure transmitter were stationed in the opposite corner of the tank from the testing platform and were connected using ¼-inch plastic tubing. For the piezometer, there was approximately 16.5 feet of tubing along the floor of the tank before ascending vertically with a 90° bend. It was in this vertical section of the tubing that the piezometer readings were made. The pressure transmitter was located about 7 inches above the vertical 90° bend of the ¼-inch plastic tubing. The actual pressure measurement taps for the piezometer, pressure transmitter and the flush mount transducer itself were all positioned to be at the center of the falling jet and orthogonal to the direction of the jet flow. The flush mounted transducer and tap for the piezometer and pressure transmitter were installed in different spots on the same plexiglass platform. The platform could be rotated to switch between the flush mounted transducer and the tap. The same tap and plastic tubing were used for both the piezometer and the pressure transmitter. The nozzle was adjusted laterally ever so slightly if needed to ensure that the jet impact was exactly centered over the instrumentation measurement point after a new instrument was rotated into position prior to testing.

Within the vertical leg of the nozzle piping immediately downstream of the last elbow, the supply line was extended by adding different lengths of 3" PVC pipe to achieve the three different fall heights. The fall heights of the jet were set to be exactly 2, 5, and 10 feet. This fall height is the vertical measurement between the end of the nozzle and the horizontal measurement platform.

Laboratory tests were performed by following these steps:

1. The piezometer and transmitter tubing were flushed before any testing using the piezometer or transmitter was completed. A garden hose with plastic tubing connected to the end was directed with a very minimal flow rate at the testing tap for the piezometer and transmitter. This flushed water through the tubing going across the floor of the concrete tank pushing air out of the lines. The plastic tube line was disconnected after the

90° vertical bend. While water flowed out of the bend, the end of plastic tubing line leading to the transmitter was held upwards and filled with the water flowing from the bend. This was done to avoid any air bubbles from being trapped in the transmitter or tubing. A similar procedure was followed to flush the line before any piezometer tests were performed.

2. Before transducer or transmitter tests were conducted, a zero reading was recorded for each instrument using the StrainSmart data acquisition system. Electrical components of test setup, including the StrainSmart, instrumentation power source, and laptop, were powered up for approximately 5-10 minutes before taking a zero reading for the transducer or transmitter. Any water sitting on the testing platform and instrumentation was cleaned off before zero readings were taken.
3. The valves in the supply piping were opened to increase the flowrate until water exited the ball valve at the highest point in the supply pipeline previously mentioned. This ensured a full pipe throughout the testing. The ball valve was closed for the remainder of tests on a given day.
4. The electrical components were on with water running for approximately 10-20 minutes before any testing was completed. This was done to avoid any misleading signals from affecting test data while temperatures stabilized due to electronic startup and the water temperature of the jet.
5. Particularly after fall heights were changed, a low flowrate of approximately 50 gpm was set to visually inspect that the jet was centered over the instrumentation in the test platform. The nozzle was adjusted as needed to center the jet.
6. The flowrate for a given test was set using the 6-inch and 8-inch valves. The nominal flowrates for testing were 50, 150, 200 and 225 gpm. The actual flowrates are shown in the RESULTS section and Tables C-1 through C-9 in Appendix C – Tabular Pressures Under a Falling Jet. All flowrates were set within $\pm 5\%$ of the target flowrate.

7. The temperature of the water at the exit of the nozzle was recorded.
8. For transducer and transmitter tests, data were recorded using the StrainSmart hardware and applicable software. The output was recorded for approximately 1 minute at 200 Hz. Other configurations of test duration and recording frequency were also completed as noted in the Discussion section.
9. For piezometer tests, the increased height of the water column was measured. The height of the water column when no water was impinging the tap was used as the datum.
10. The diameter of the jet at impact was measured using calipers. The diameter was measured approximately 2-4 inches above the test platform. The diameter was measured 4 times at every 45° around the jet. The impact diameter was measured for all configurations of fall height and flow rate.
11. Photos and video recordings were taken for all configurations of fall height and flowrate.

Calculated Impact Force

The force at the impact point of the falling jet was estimated by using a relationship between momentum and force. A body of water with some velocity has momentum. The momentum is converted to a force when it is deflected off another object by the relationship shown in Equation 1 (Nazeer Ahmed 1987).

$$F = -\rho Av^2(\cos\theta - 1) \quad (\text{Equation 1})$$

F – force orthogonal to the solid, physical boundary

ρ – density of water

A – cross-sectional area of jet

v – jet velocity

θ – angle of impact to solid, physical boundary

The angle of impact was orthogonal to the solid physical boundary. The water temperature used to determine the density of water was 40 °F. These calculations do not include the effect of air drag, air bulking, or jet dissipation on the falling jet. The flow continuity equation as shown in Equation 2 was used to substitute the cross-sectional area of the jet and impact velocity in Equation 1 for the flow rate of the jet (Nazeer Ahmed 1987).

$$Q = vA \quad (\text{Equation 2})$$

Q – flow rate of the jet

v – jet velocity

A – cross-sectional area of jet

The impact velocity was calculated based on kinematics as shown in Equation 3 (Lewis et al. 1999).

$$v_i = \sqrt{v_o^2 + 2gH} \quad (\text{Equation 3})$$

v_i – jet velocity at the impact point on a solid boundary

v_o – initial jet velocity

g – acceleration due to gravity

H – fall height of jet

The impact velocity from Equation 3 is the velocity used in Equation 1 to calculate the impact force.

Computational Fluid Dynamics Simulations

In addition to laboratory tests and calculated values, the lowest flow rate during laboratory tests was simulated at the three fall heights in computational fluid dynamics using Starr CCM+ software. The laboratory test data used for comparison was the pressure transmitter at approximately 4.76 fps. The details for test duration and data collection frequencies for different fall heights are summarized in Table 1.

Table 1 – CFD simulation data collection frequency.

	Fall Height (ft)		
	2	5	10
Frequency (Hz)	100-1000	3.125-200	16.7-200

RESULTS

Laboratory Tests

The resulting impact pressure for various fall heights and flowrates are plotted below where the abscissa is initial velocity. The initial velocity is defined as the velocity at the tip of the nozzle as calculated by the measured flow rate and the inside diameter of the nozzle itself. Though impact velocity is more closely related to the impact pressure than the initial velocity is, the initial velocity was used when plotting pressure data to present the data with a measurable test variable rather than using a calculated method such as the method used when calculating force as described in the PROCEDURE section. The plots relating initial velocity to mean pressure of the jet at impact are shown in Figures 5-7.

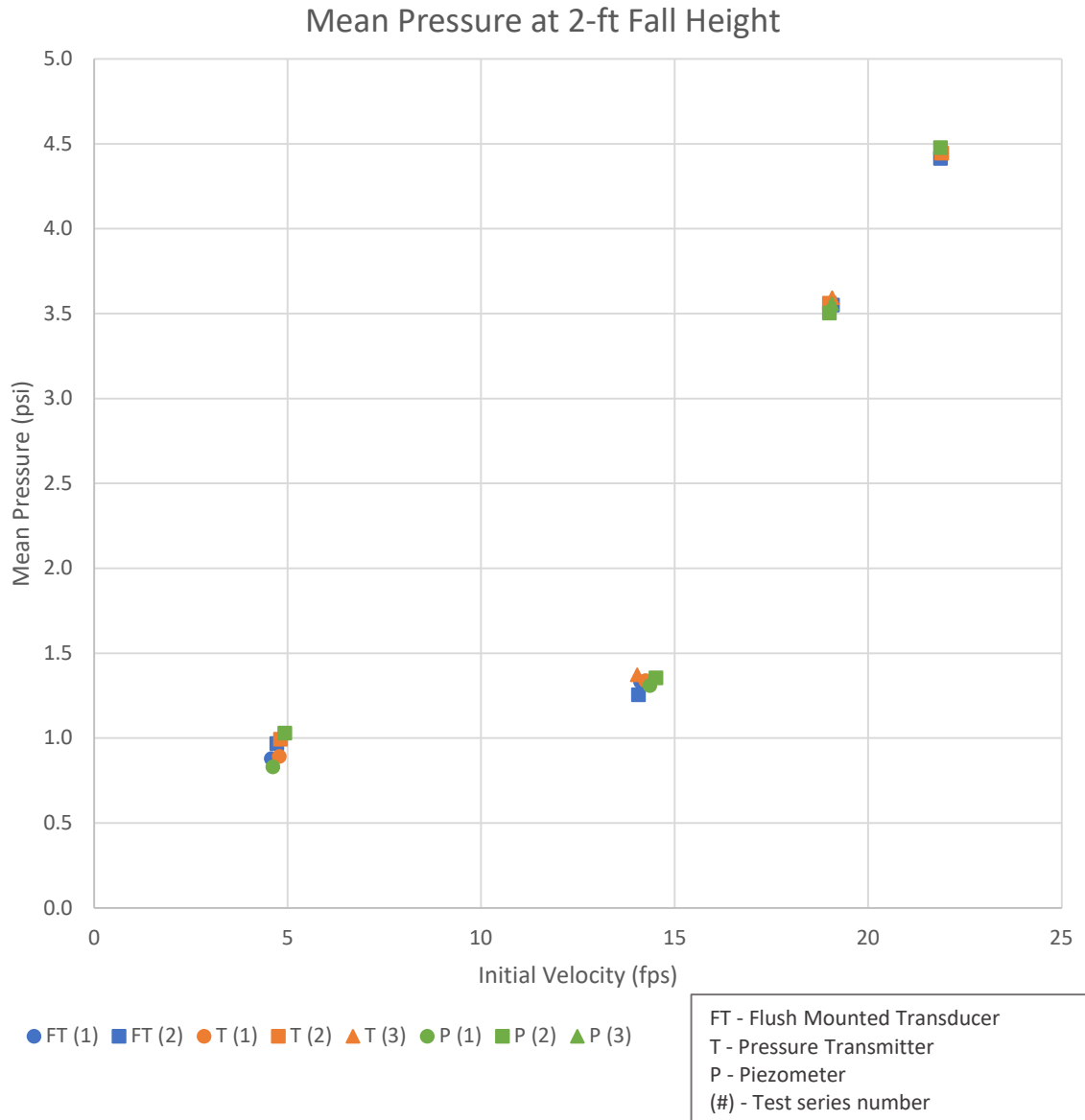


Figure 5 – Impact pressure head for various flowrates at a fall height of 2 feet.

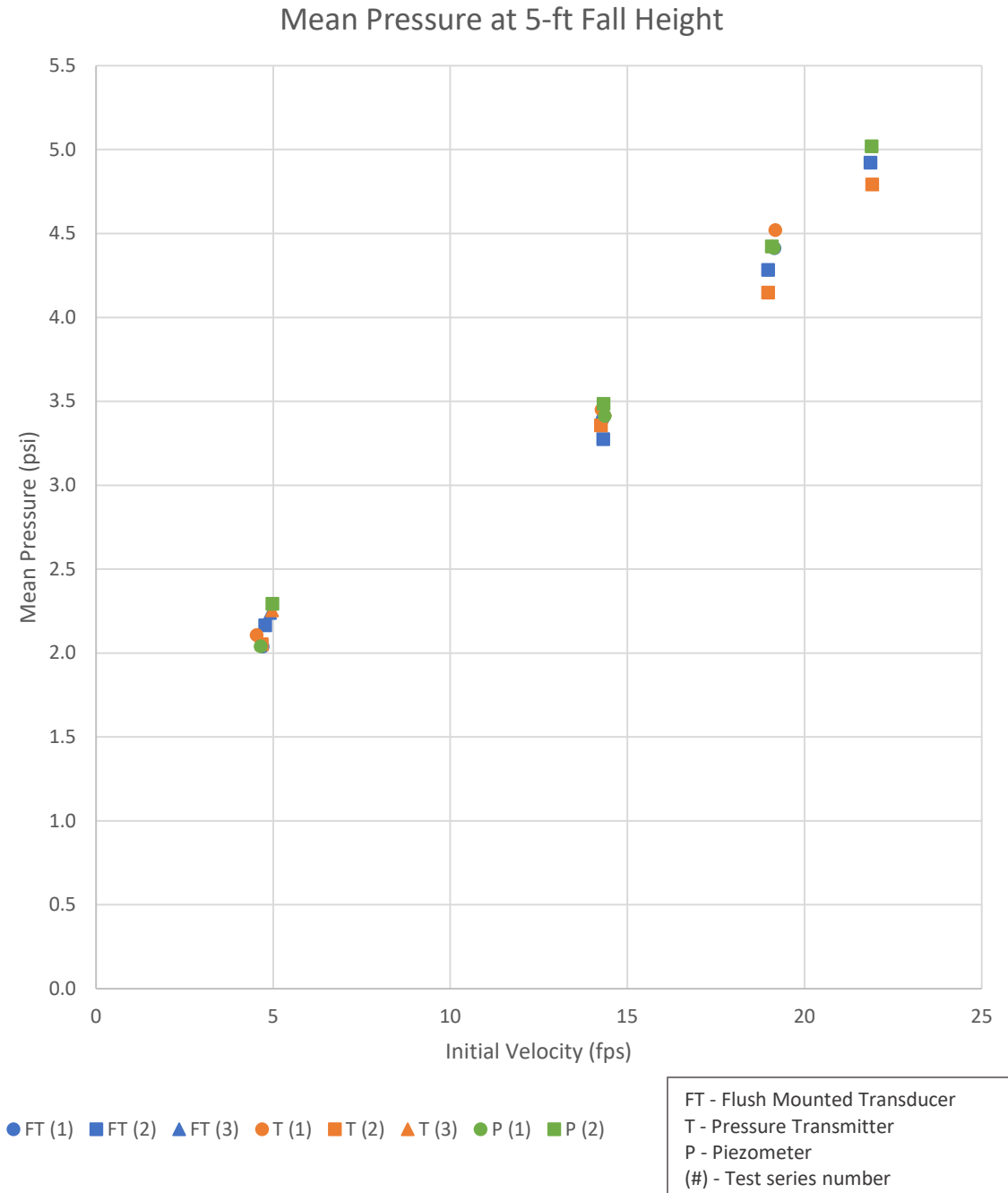


Figure 6 – Impact pressure head for various flowrates at a fall height of 5 feet.

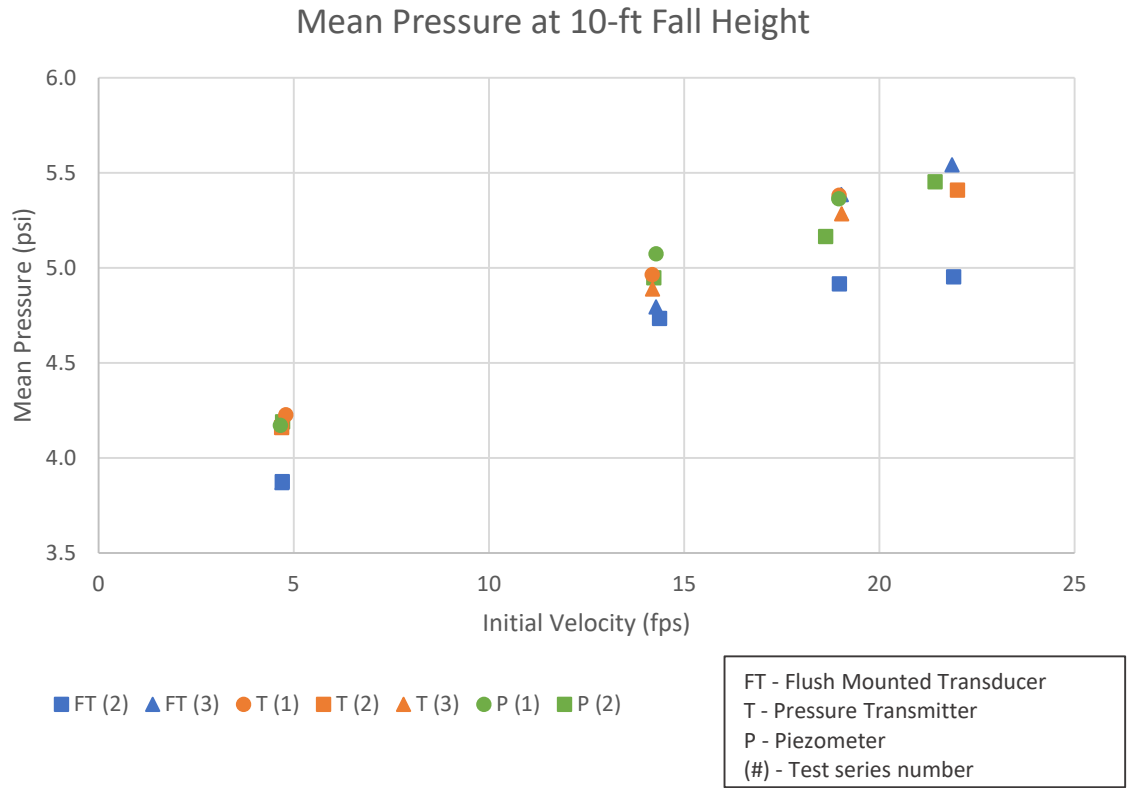


Figure 7 – Impact pressure head for various flowrates at a fall height of 10 feet.

The impact pressures recorded are also grouped in plots by method of measurement in Figures 8-10.

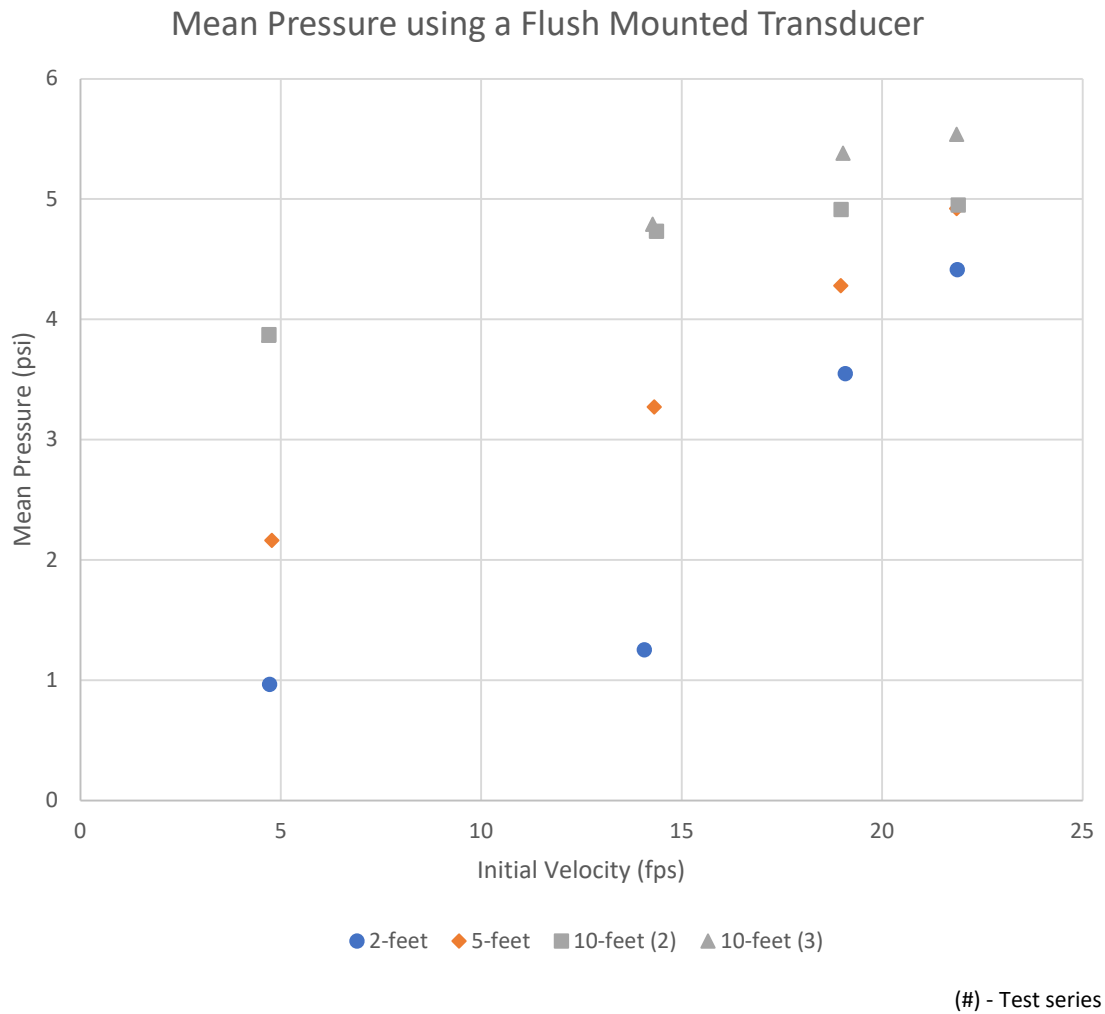


Figure 8 – Impact pressure head for various flowrates using a flush mounted transducer.

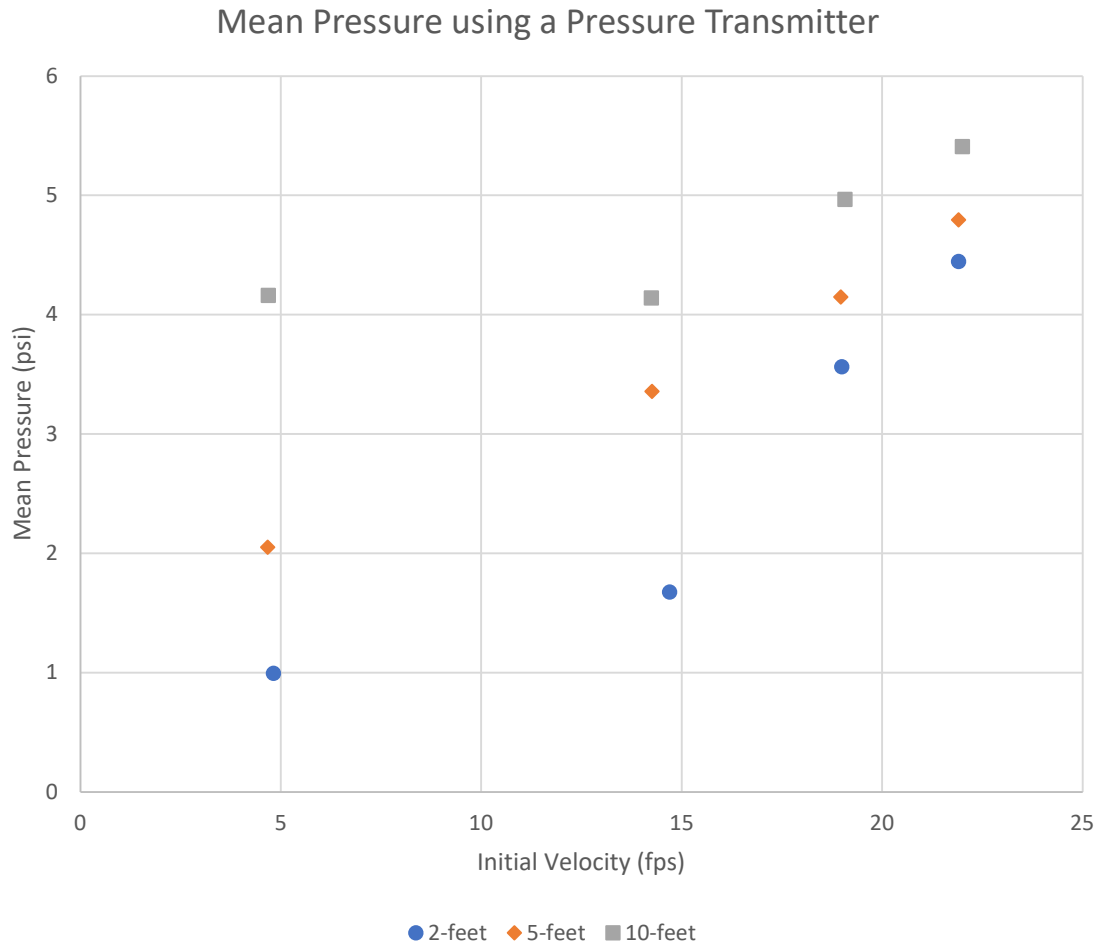


Figure 9 – Impact pressure head for various flowrates using a pressure transmitter.

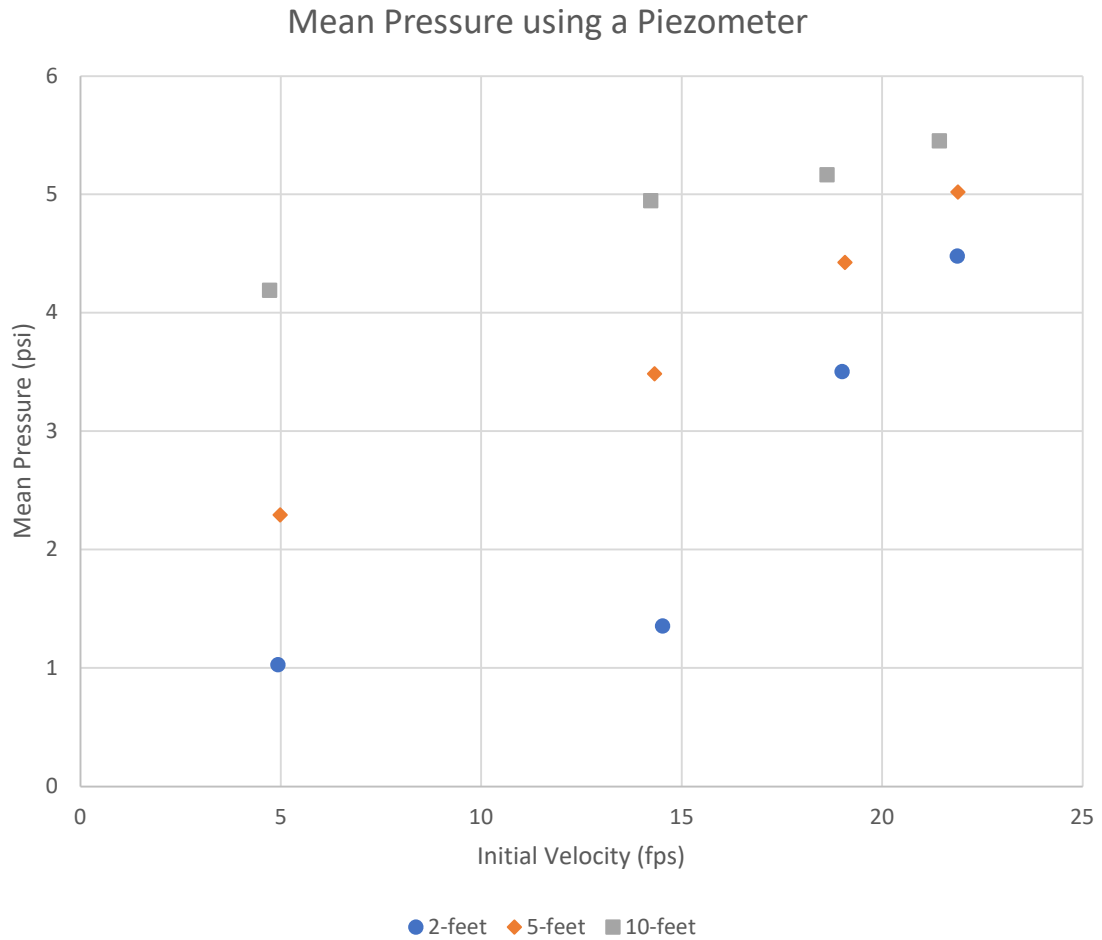


Figure 10 – Impact pressure head for various flowrates using a piezometer.

The diameter of the jet at impact was measured approximately 2-4 inches above the test platform.

The impact diameter is plotted against the initial jet velocity (the velocity of the water jet as it leaves the nozzle) for the various fall heights in Figure 11. Observations made about the data in Figure 11 can be found in the DISCUSSION section.

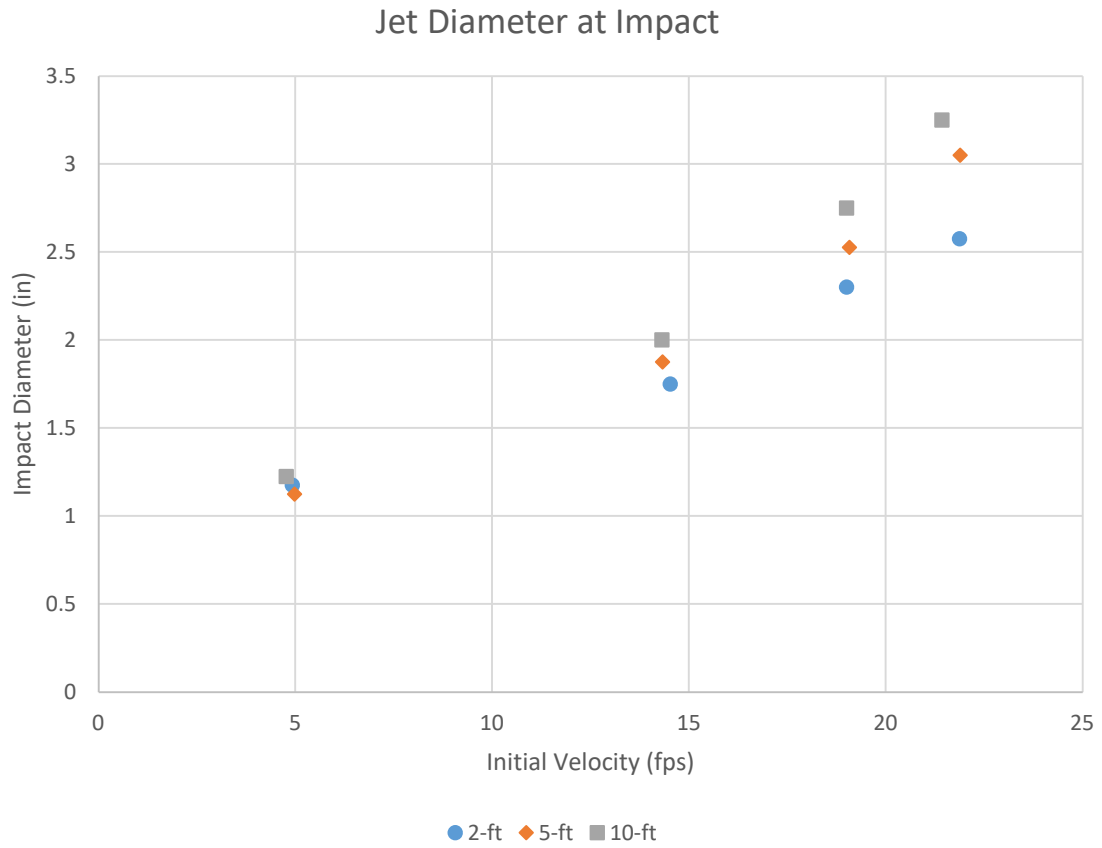


Figure 11 – Jet diameter at impact for various flowrates and fall heights.

The percent air in the jet at impact was calculated using the impact diameter. The percent air is plotted against initial jet velocity for various fall heights in Figure 12. Observations made about the data in Figure 12 can be found in the DISCUSSION section.

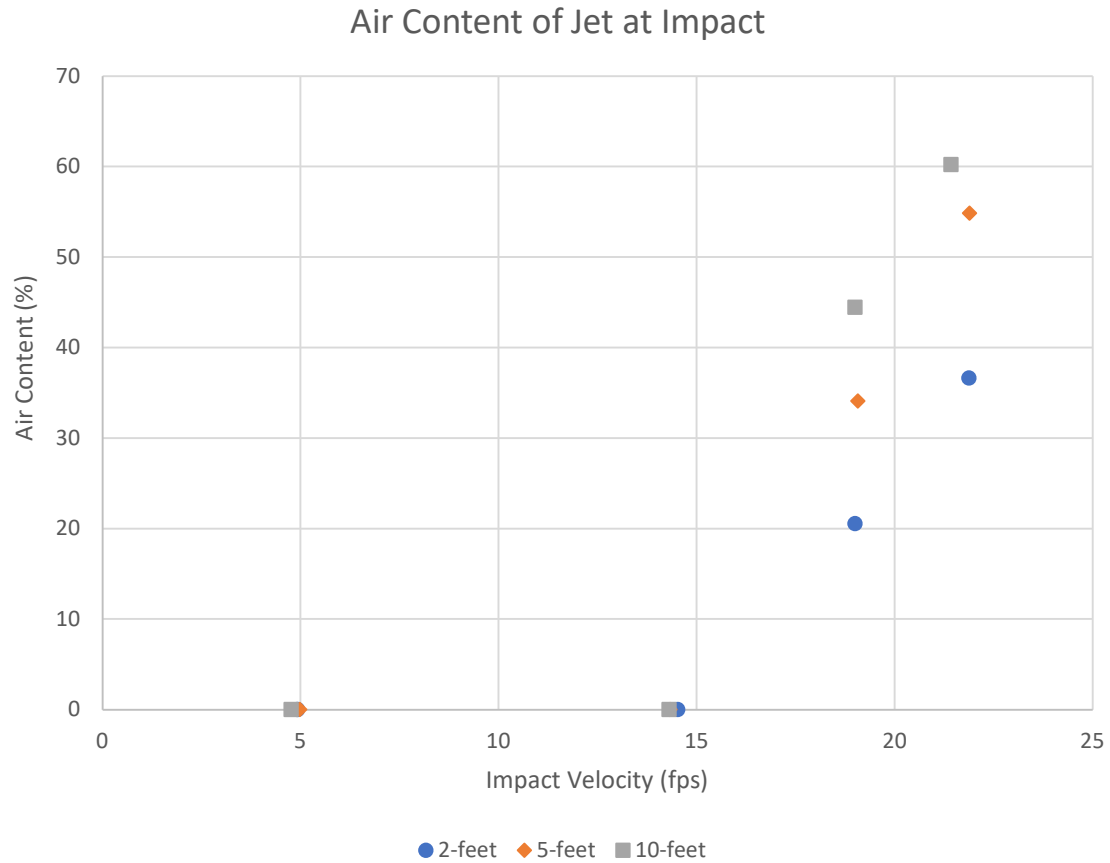


Figure 12 – Percent air content at impact for various flowrates and fall heights.

The air content of the jet at impact was estimated based on the impact jet diameters shown in Figure 11. It was assumed that little to no air aspirated into the water supply line during the laboratory tests. The inside diameter of the pipe was used as the initial diameter of the jet. The jet was assumed to have little to no air content when exiting the nozzle, i.e. the initial flow area of the jet was all water and little to no air.

During these tests, the flow area was calculated again based on the measured jet diameter at impact. Any decrease in the flow area was assumed to be associated with the acceleration of

gravity. Any increase in the flow area was directly correlated to an increase in air content in the jet. The air content shown in Figure 12 is a percent of the total flow area on impact.

The jet diameter at impact was less than or equal to the initial jet diameter, which was 2.05 inches, for the two lower flow rates. Consequently, any test run at these flow rates was noted as having no air content at impact, as shown in Figure 12. The two higher flow rates had air content at impact.

Calculated Impact Force

In addition to laboratory measurements, the forces at impact were calculated using equations of momentum and plotted against fall height as shown in Figure 13.

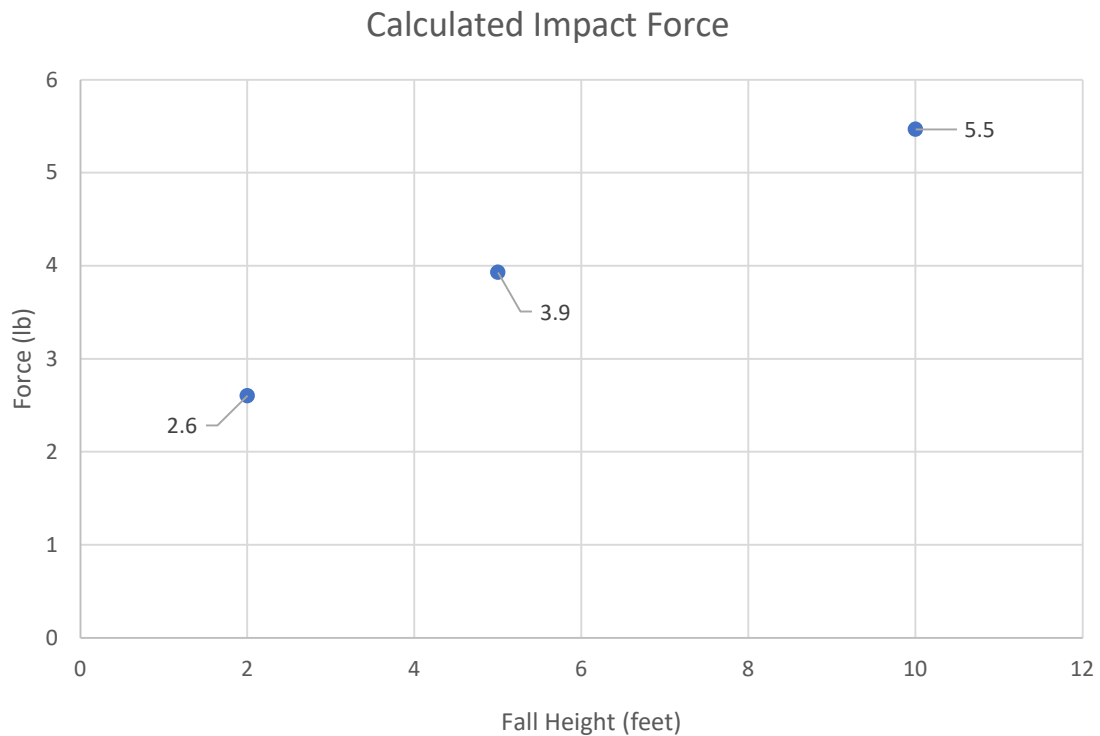


Figure 13 – Impact force calculated with equations of momentum.

The initial velocity of the jets shown in Figure 13 were approximately 5 fps. The impact force calculated for the 2-foot, 5-foot, and 10-foot fall heights were 2.6 lbs., 3.9 lbs., and 5.5 lbs., respectively. The data presented in Figure 13 is discussed further in the DISCUSSION section.

Computational Fluid Dynamics Simulations

Instantaneous pressure at the impact point for the portions of the CFD simulations and corresponding graphs from laboratory tests using a pressure transmitter under a column of water for an initial velocity of 4.76 fps are shown in Figures 14-22. For all three fall heights, more pressure fluctuation is recorded by laboratory tests. For example, in the 2-foot fall height, the range of pressure for laboratory tests was almost 0.1 psi, whereas it was only 0.002 psi for the CFD simulation. The mean pressures from CFD for the 2-ft, 5-ft, and 10-ft fall heights were 0.92, 2.13, and 3.86 psi, respectively.

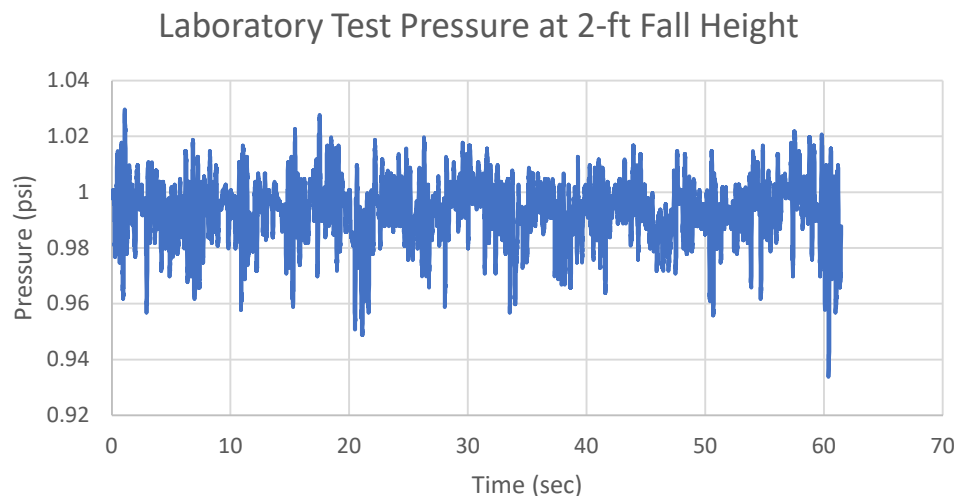


Figure 14 – Laboratory test pressure using pressure transmitter for 2-ft fall height.

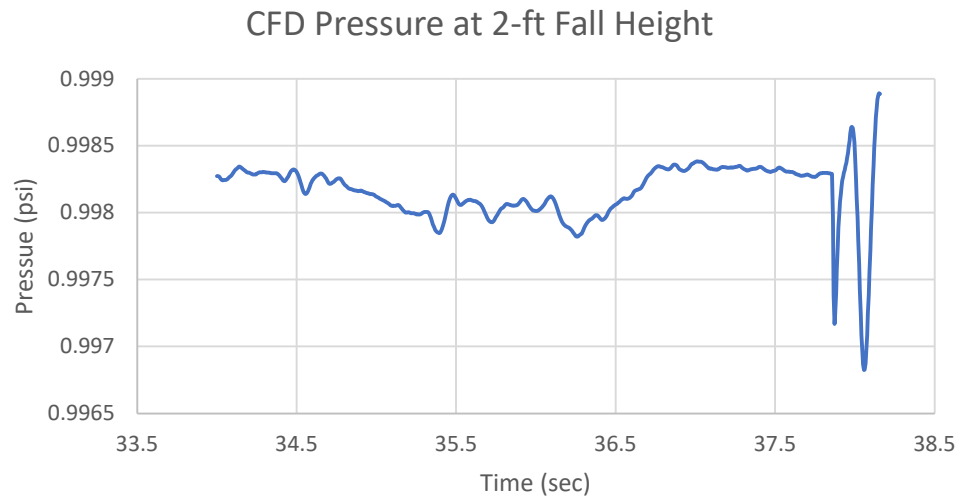


Figure 15 – CFD pressure data plotted over time for 2-ft fall height.

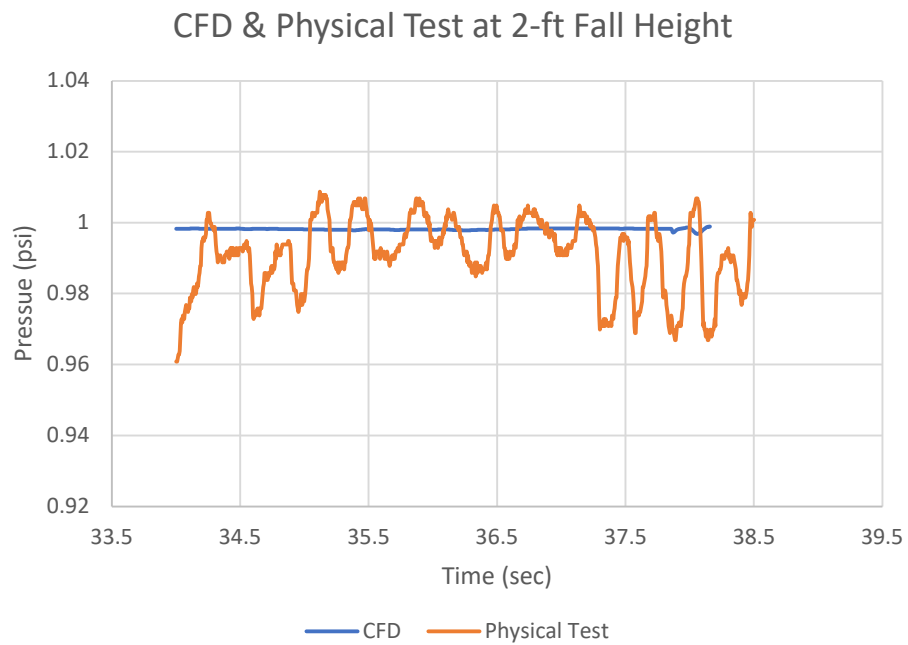


Figure 16 – Sample of CFD and physical test data at 2-ft fall height.

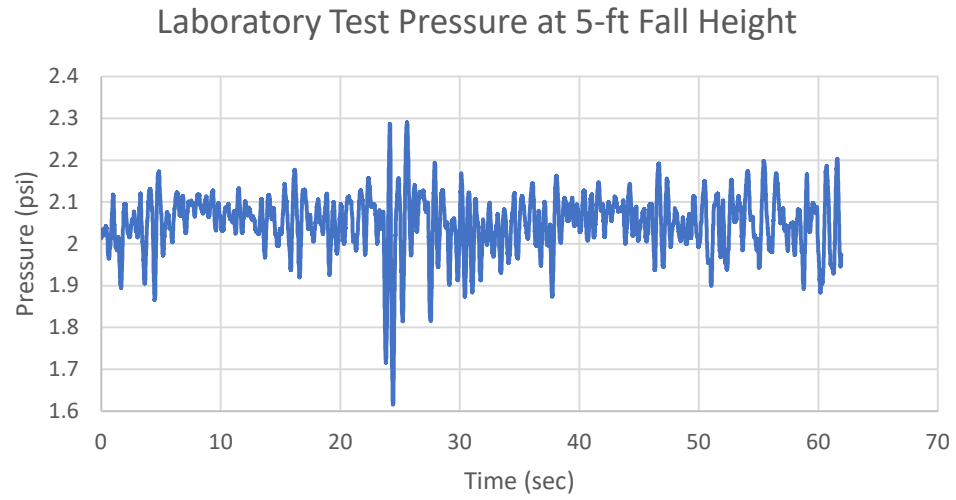


Figure 17 – Laboratory test pressure data using pressure transmitter for 5-ft fall height.

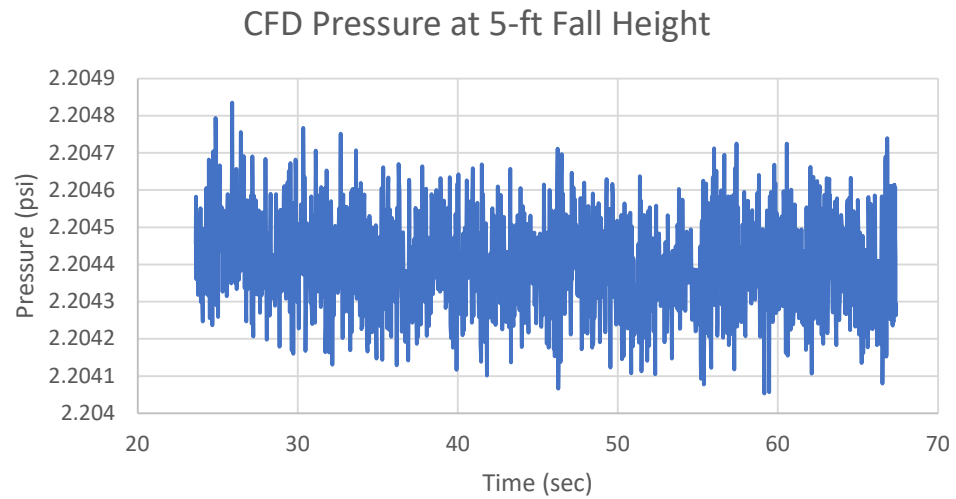


Figure 18 – CFD pressure data plotted over time for 5-ft fall height.

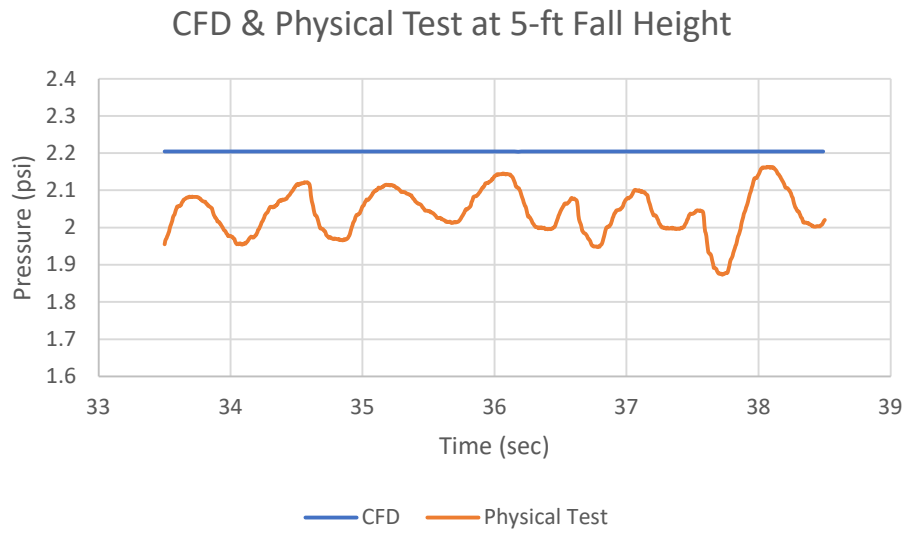


Figure 19 – Sample of CFD and physical test data at 5-ft fall height.

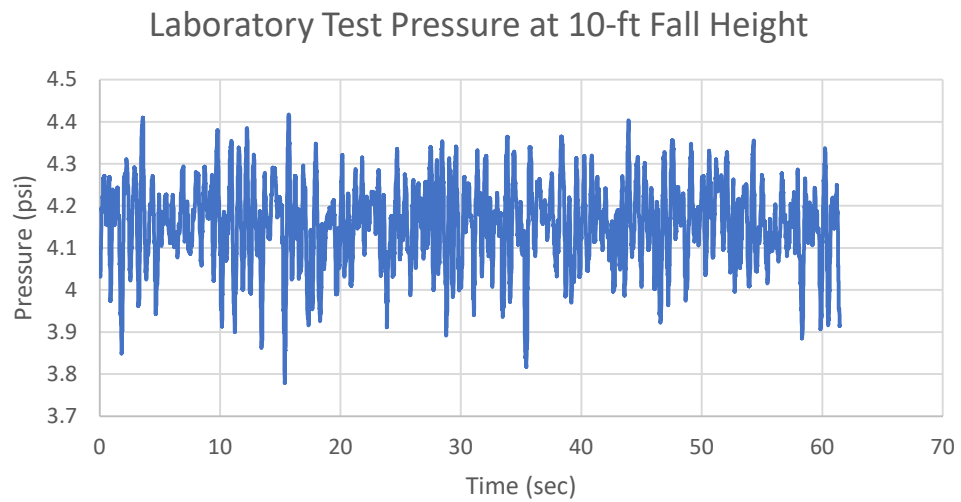


Figure 20 – Laboratory test pressure data using pressure transmitter for 10-ft fall height.

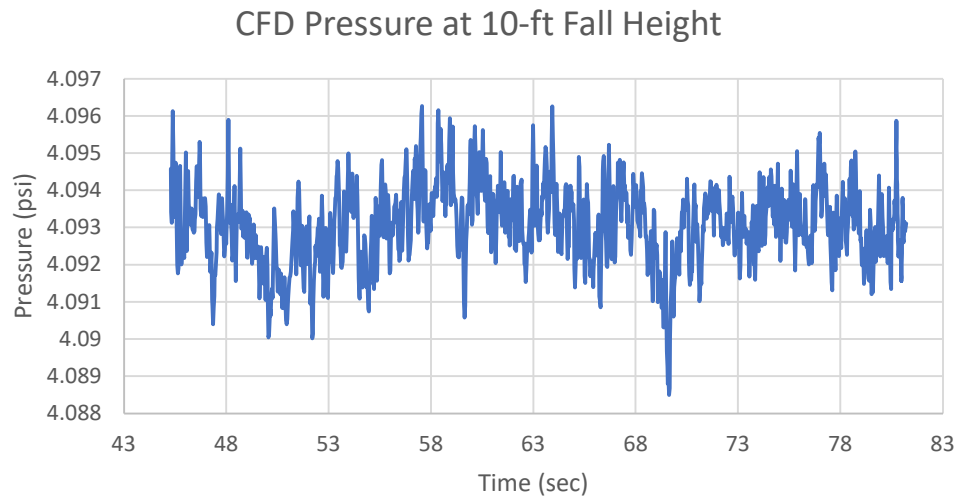


Figure 21 – CFD pressure data plotted over time for 10-ft fall height.

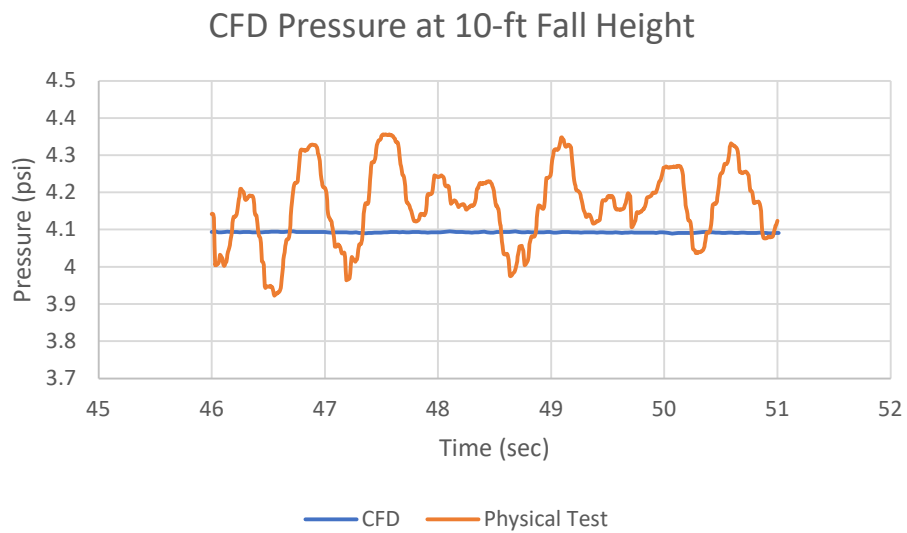


Figure 22 – Sample of CFD & physical test data at 10-ft fall height.

Only portions of the CFD were taken at a time step that represented data taken at 200 Hz, which was the frequency that the laboratory data was taken at. The resultant force on the testing platform in the CFD model was also recorded. The forces for a jet with an initial velocity of approximately 5 fps at three different fall heights are shown in Figure 23. The data presented in Figure 23 is discussed further in the DISCUSSION section.

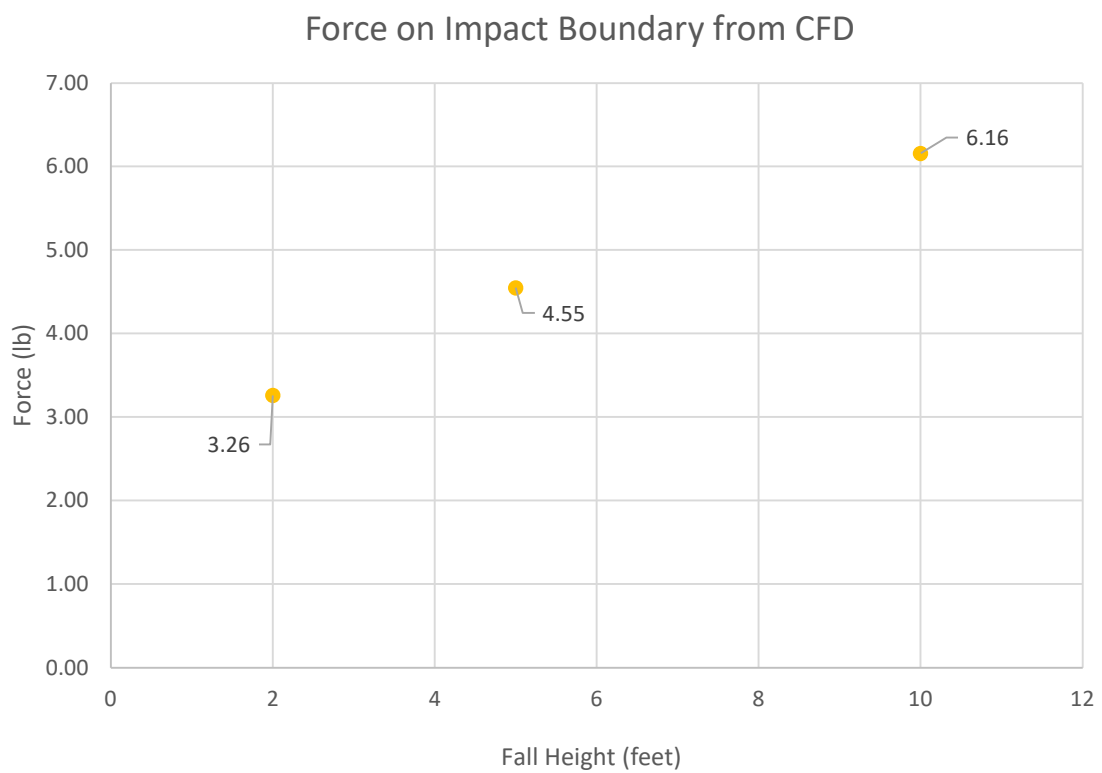


Figure 23 – Force on solid, impact boundary from CFD model.

Results Summary

The pressure data resulting from laboratory testing, CFD simulations, and Fathi et al. values are plotted in Figures 24-26 for the 2-, 5-, and 10-foot fall heights.

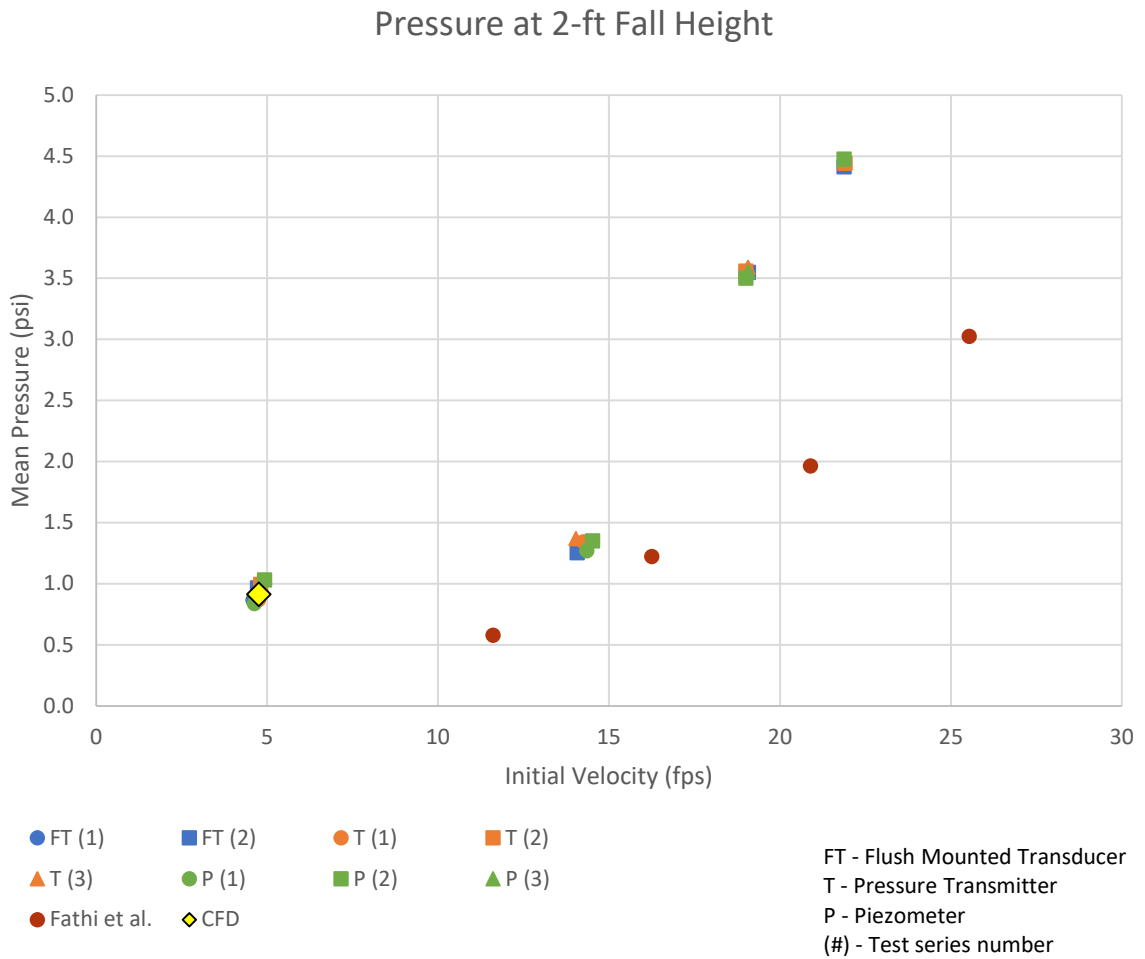


Figure 24 – Pressure data from various sources for a 2-ft fall height.

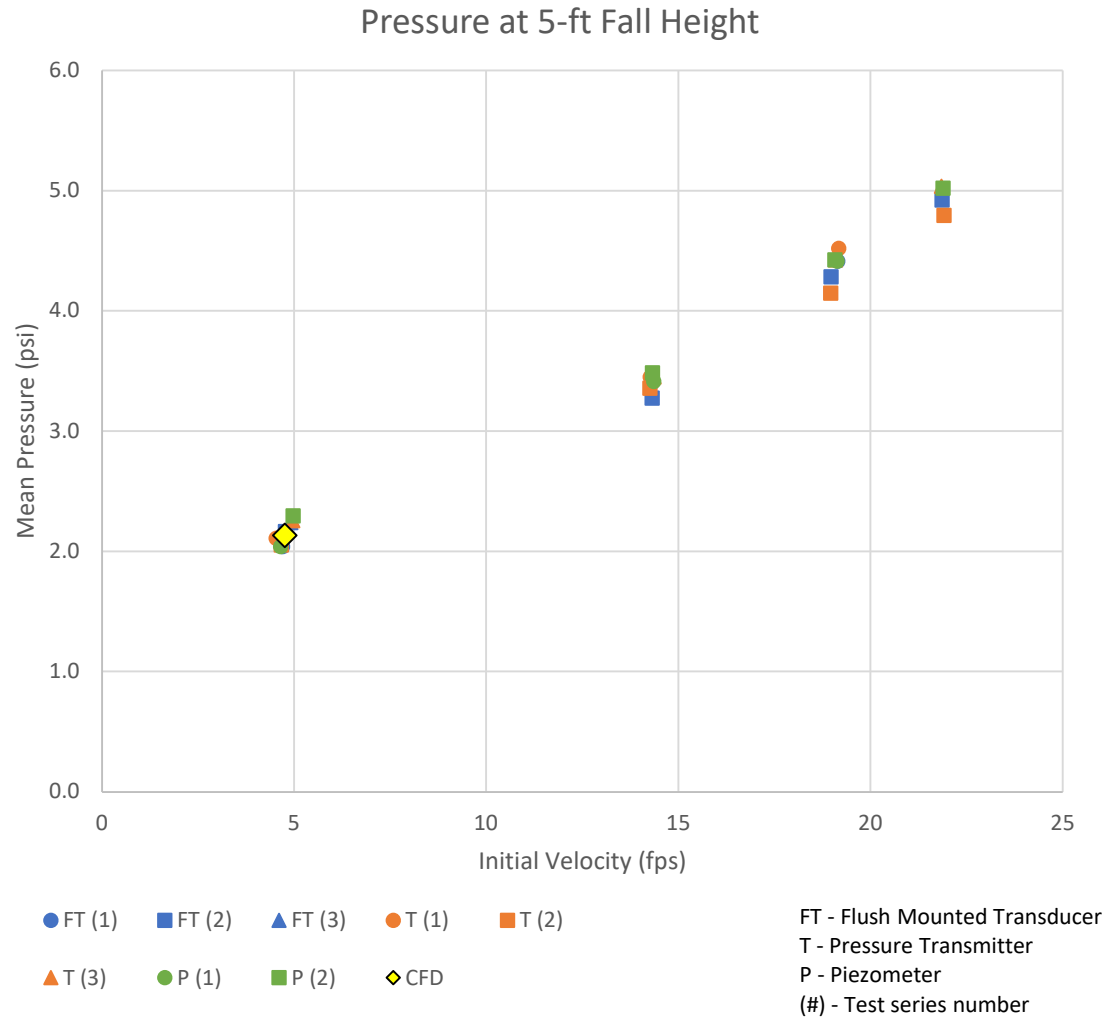


Figure 25 – Pressure data from various sources for a 5-ft fall height.

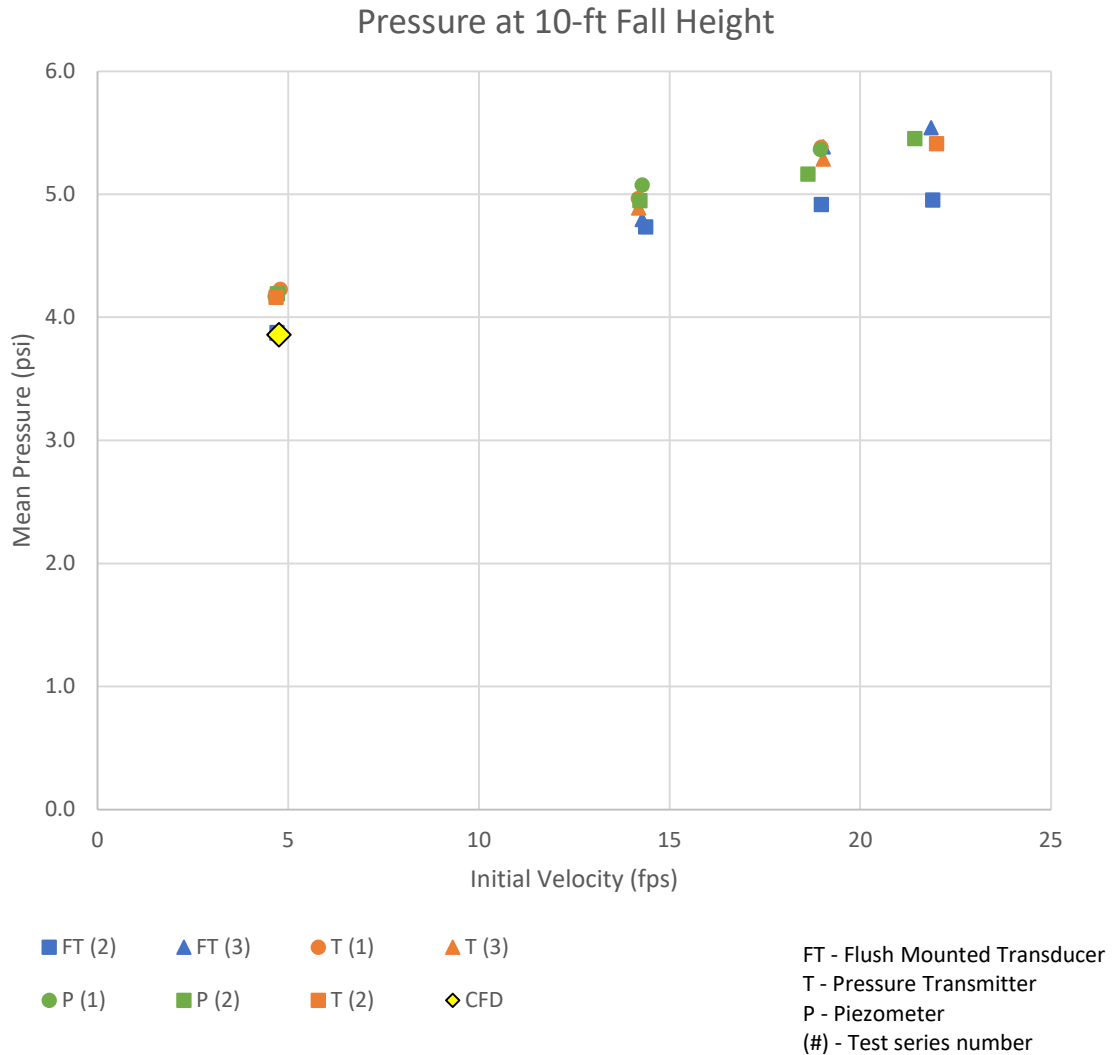


Figure 26 – Pressure data from various sources for a 10-ft fall height.

DISCUSSION

An analysis of the results was completed by noting patterns within data grouped by fall height and by method of measurement. Results and observations from laboratory tests, calculated pressures, and CFD simulations are discussed in this section. The discussion on results from

laboratory tests include observations regarding a comparison of laboratory test data and data from the study completed by Fathi et al. Potential sources of error, repeatability, and other variables in testing are also discussed.

Laboratory Tests at a 10-ft fall Height

The pressures recorded during testing were plotted against the initial velocity of the jet. This relationship was analyzed for the various measurement methods at different initial velocities. The following observations were made for laboratory tests at a 10-ft fall height:

1. The two repeat tests for the flush mounted transducer at the 10-foot fall height and 19 fps were all different and were found to be unrepeatable. The resulting data spanned a range of approximately 0.62 psi. The highest point matched the pressure transmitter and piezometer pressures within approximately 0.25 psi. The pressure at this height and velocity seems to fall within a range of pressures.
2. The two higher velocity runs recorded for the flush mount transducer at the 10-foot fall height exhibit milder slopes than the two lower velocity runs as shown in Figure 27. The sections where this is most prominent in the plot are labeled A and B in Figure 27. These two test-series are the second and third iterations for this flow rate and fall height, labeled FT (2) and FT (3) in Figure 27.

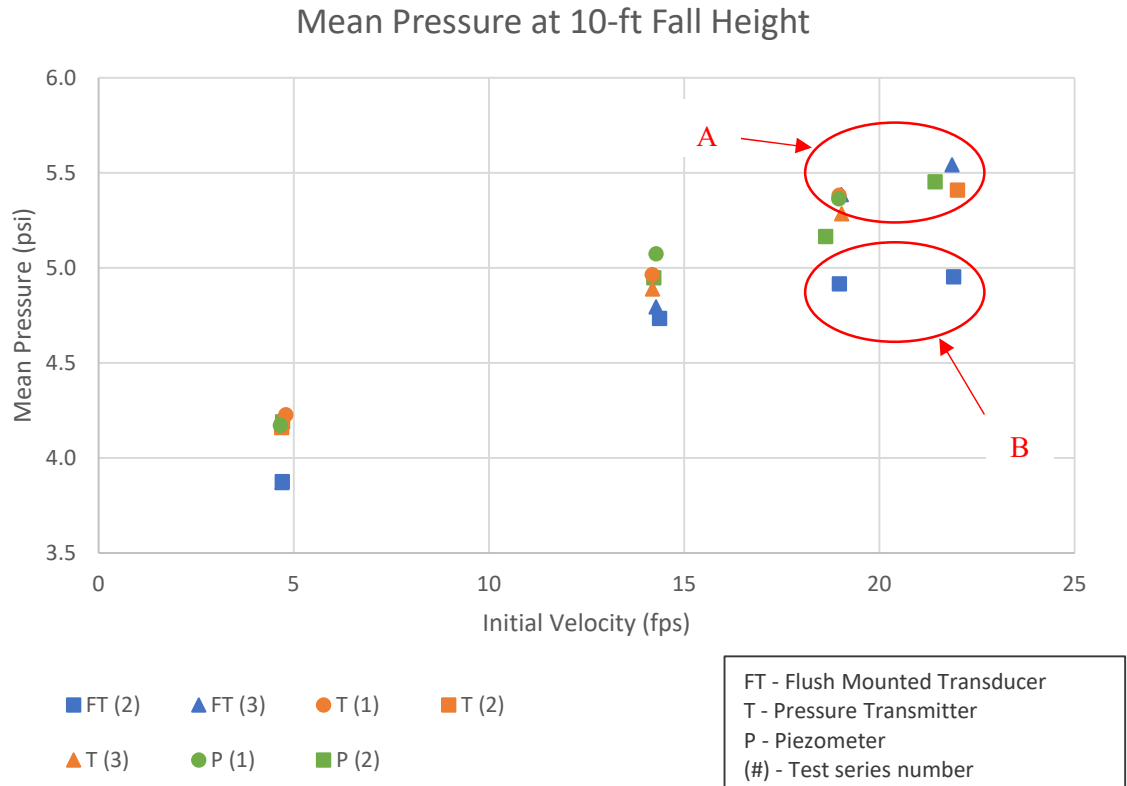


Figure 27 – Impact pressure head at a fall height of 10 feet (with annotations).

For the run labeled FT (2) in Figure 27, the mean pressure only increased by 0.03 psi for an increase in initial velocity of 2.92 fps between the two tests at the highest initial velocity in the detail labeled B in Figure 27. The slope of the line decreases as velocity increases for the pressure transmitter and piezometer recordings.

Laboratory Tests at a 5-ft fall Height

The pressures recorded at the 5-foot fall height among the different methods of measurement showed less variation than at the 10-ft fall height. All the tests recorded pressures within a range of approximately 0.25 psi for a given initial velocity. The tests recorded at the 5-foot fall height

are shown in Figure 6. The pressures recorded at the 5-foot fall height display the most consistent slope between impact pressure and initial velocity among the different fall heights.

Laboratory Tests at a 2-ft fall Height

The pressures recorded at the 2-foot fall height were generally consistent between the three different modes of physical measurement. The jets at this fall height had less fall time to create a developed jet. In addition, any turbulence that existed in the flow had less time to entrain air while falling.

Other Observations for Laboratory Tests

The range of pressures for the 2-, 5-, and 10- foot fall heights were approximately 3.61, 3.00, and 1.67 psi, respectively. These three ranges of pressures are the difference between the maximum and minimum pressures across all methods of laboratory measurement and all flow rates for a given fall height as shown in Figures 28-30. It appears that the range of the pressures decreases as fall height increases for the laboratory data recorded.

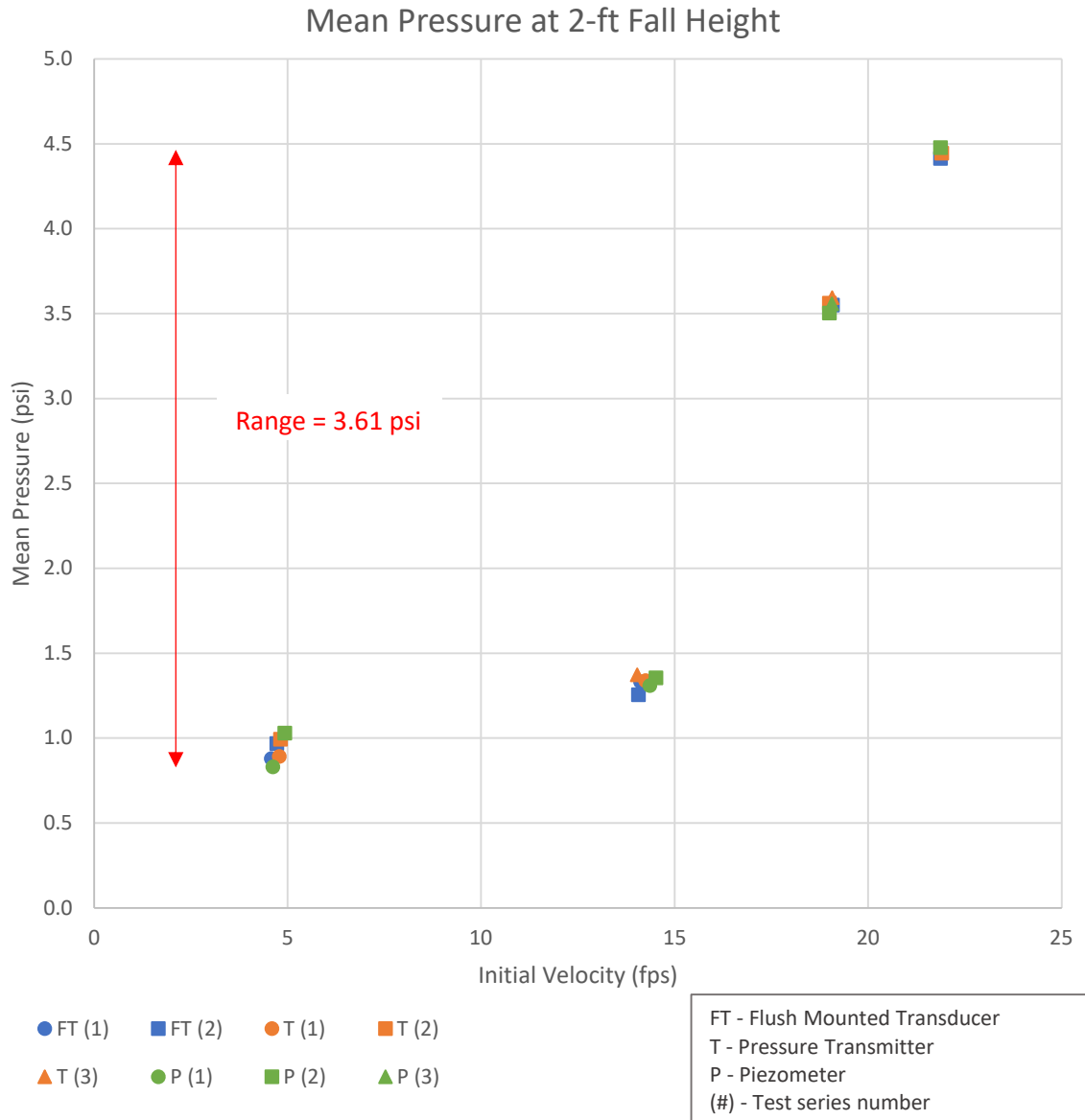


Figure 28 – Range of pressures for 2-foot fall height.

Mean Pressure at 5-ft Fall Height

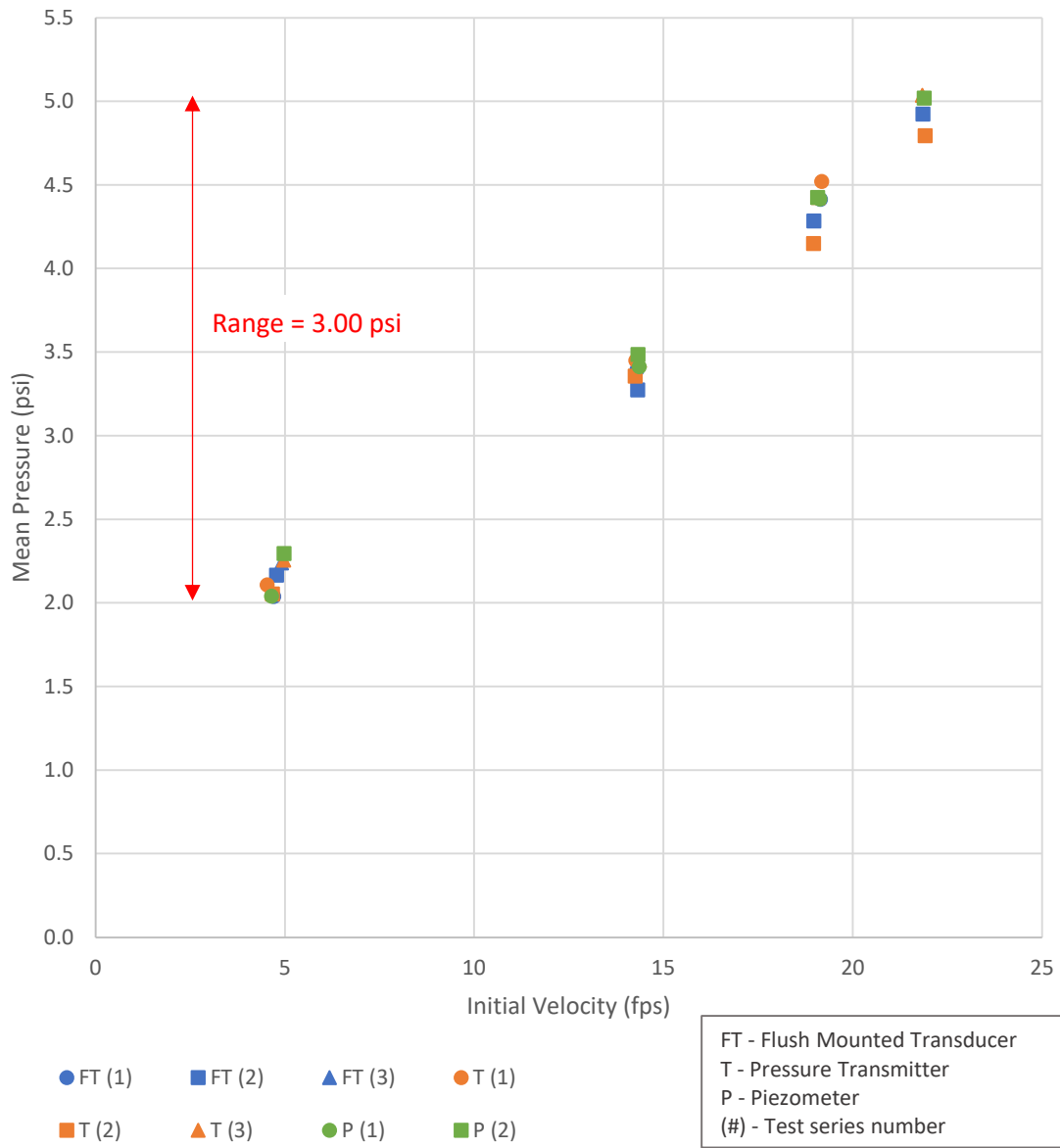


Figure 29 – Range of pressures for 5-foot fall height.

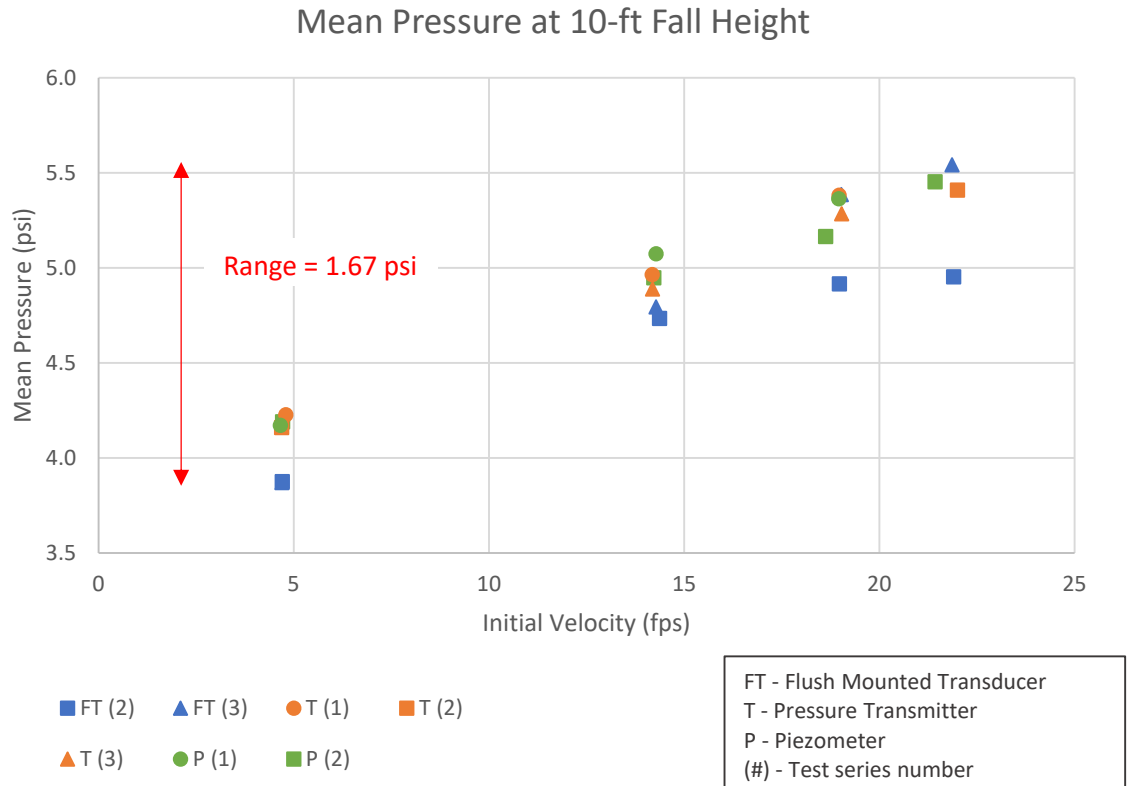


Figure 30 – Range of pressures for 10-foot fall height.

The impact jet diameter increases as initial jet velocity increases as shown in Figure 31. The diameter also increases as fall height increases for all data points except for the lowest flow rate at the 2-foot and 5-foot fall heights. For this flow rate, the 2-foot fall height jet had a larger impact diameter than the 5-foot fall height jet as shown by the area labeled A in Figure 31.

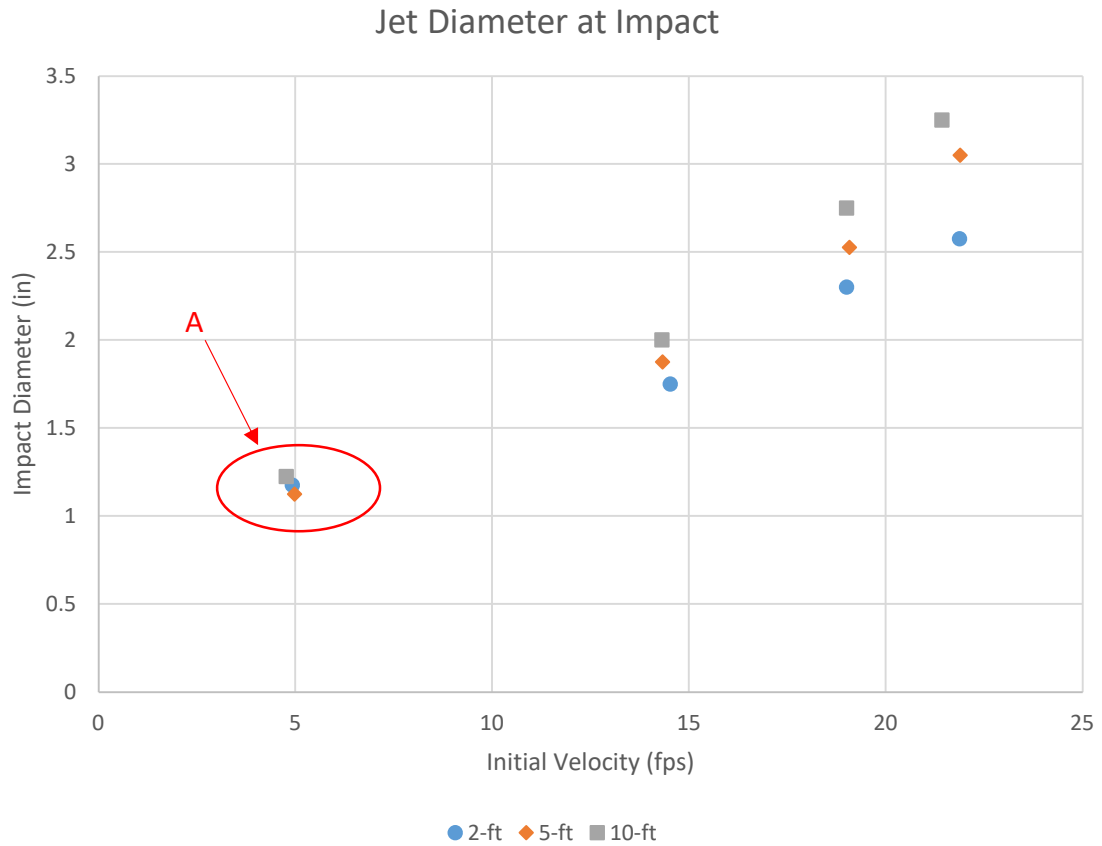


Figure 31 – Jet diameter at impact with annotations

The air content of the jet for various flow rates and fall heights is shown in Figure 32. The air content increases as velocity increases and as fall height increases. There was no air content in jets tested in the current study with an initial velocity of approximately 14 fps or lower as shown in the area labeled A in Figure 32.

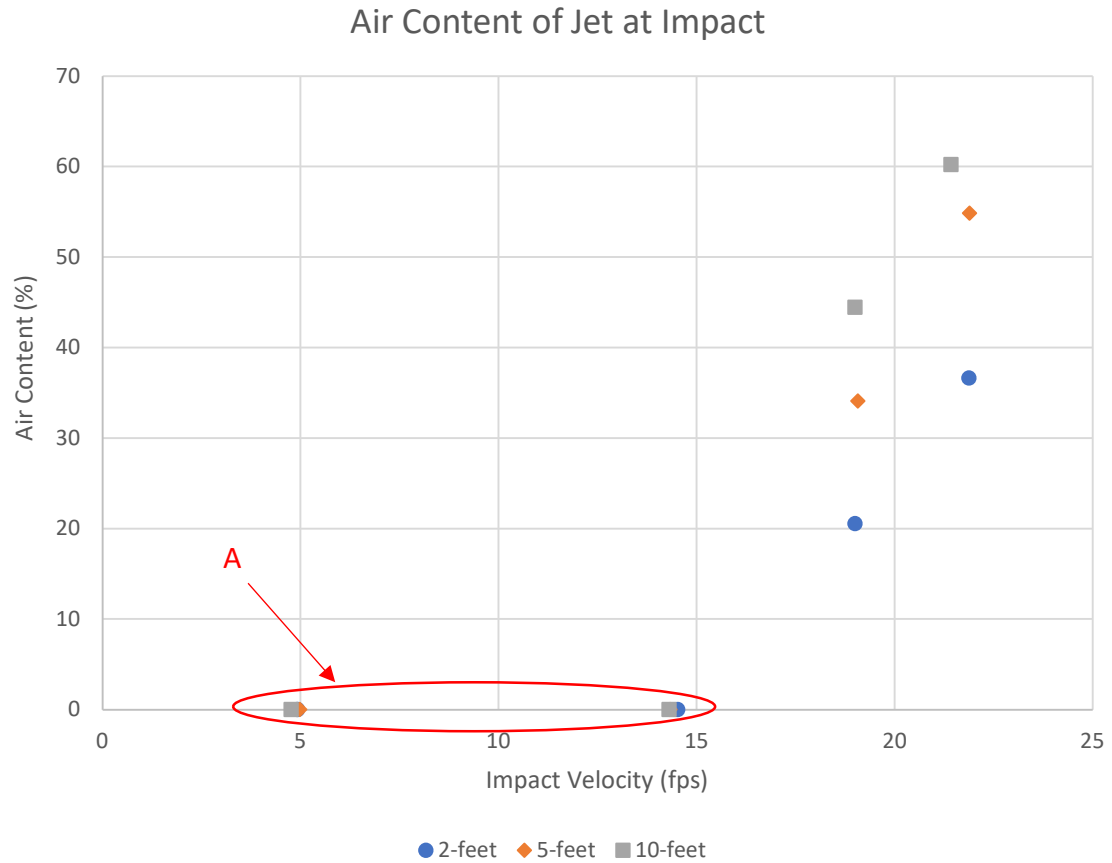


Figure 32 – Air content of jet with annotations.

Higher fall height and higher flow rates both resulted in more air entrained in the jet while falling. The higher flow rates result in increased turbulence. More turbulence results in more air entrained in the water. A higher fall height would give more time for air to be entrained by the turbulent jet. A higher velocity would decrease the amount of time for air to be entrained. The fall duration for the jet at different fall heights and flow rates are shown in Figure 33.

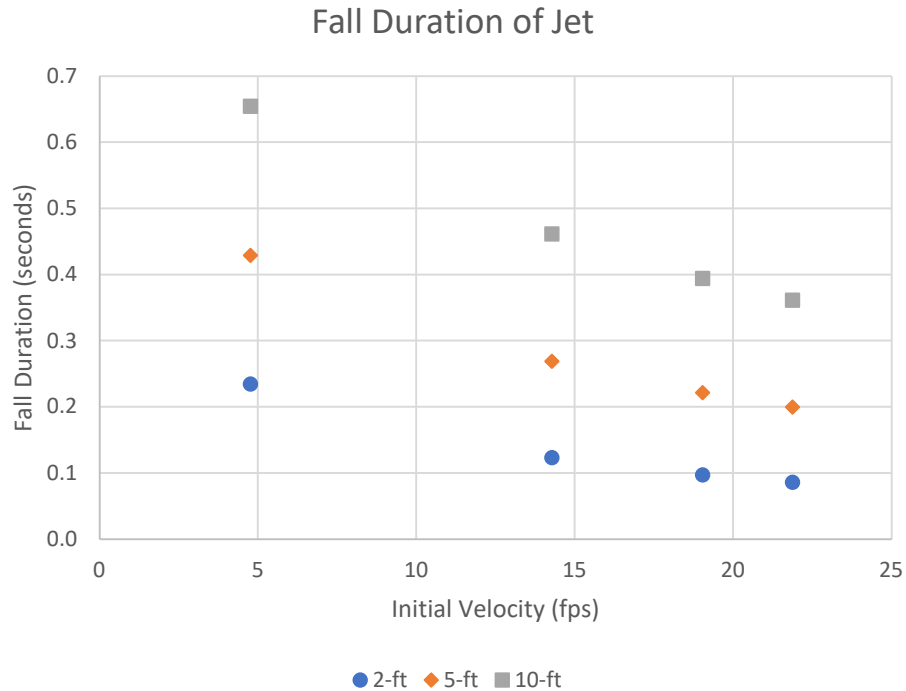


Figure 33 – Fall duration of jet for different fall heights & flow rates.

Though the fall duration decreases with increased initial velocity, the air content shown in Figure 32 increases with increased velocity. The surface area of the jet, which is greater for higher fall heights, also affects the amount of air entrained in the jet. A jet with a higher fall height has more surface area along which air can be entrained. The surface area and turbulence caused by higher velocities seem to have a greater effect on the amount of air entrained in the jet than the fall duration does.

Comparison to Previous Study

The test results were also compared to results obtained by Fathi et al. (Fathi-Moghadam et al. 2019). The tests performed by Fathi et al. were the closest experiments that were found during the literature review to the laboratory tests conducted in the current study. Fathi performed a study

where the impact pressure of a falling jet was measured. One of the test configurations was at a fall height of 60 cm (1.97 ft) and nozzle diameter of 5.1 cm (2.01 in). The method of measurement was a piezometer and pressure transmitter. The results from Fathi are compared with the results obtained for the 2-foot fall height for this study as shown in Figure 34.

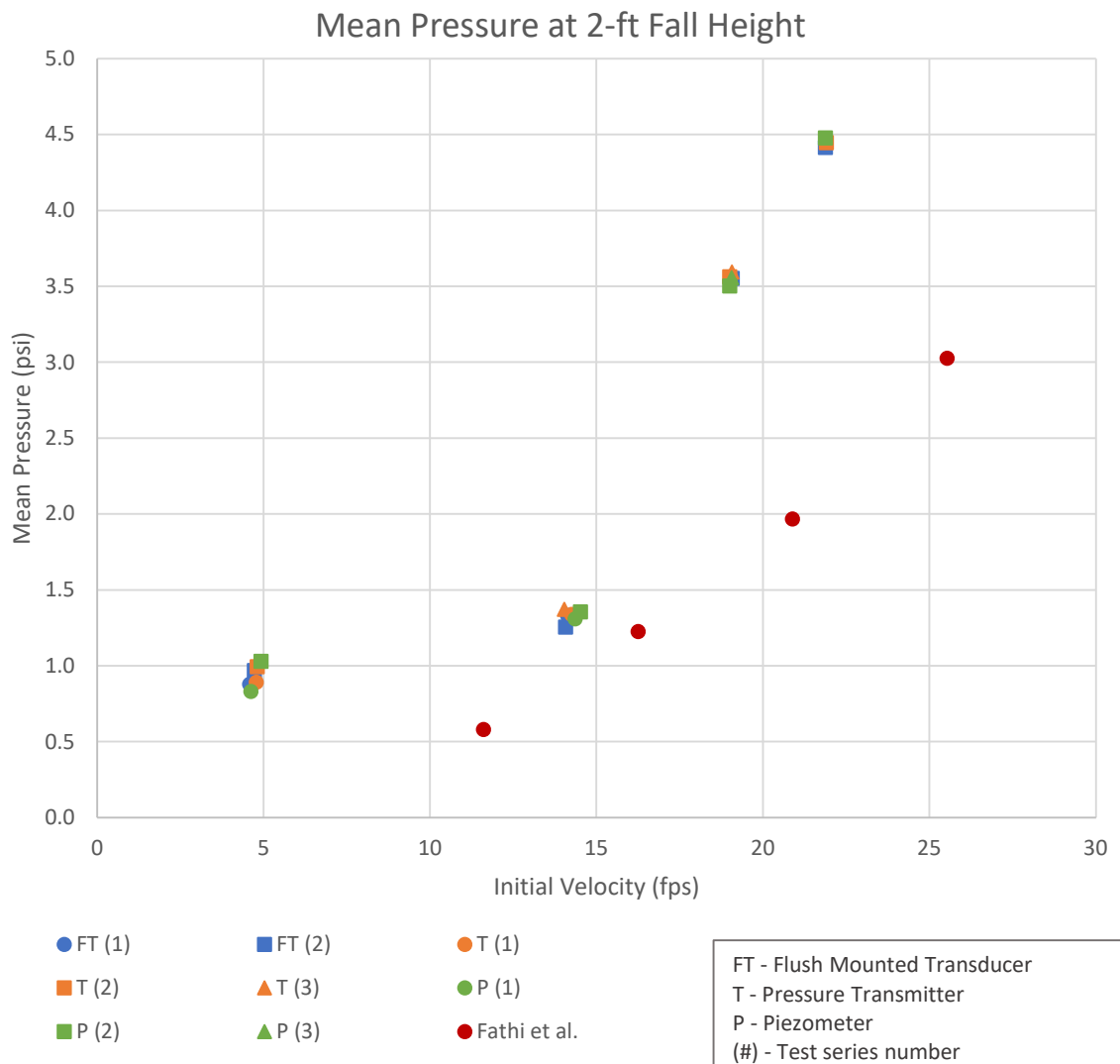


Figure 34 – Impact pressure at 2-foot fall height for this study and Fathi et al.

The resulting pressures produced by Fathi et al. are all lower than those obtained from the current study. One difference that may have produced the range in results is that Fathi used 17 taps connected to piezometers. The current study only took a reading at the center of the jet. The location of measurement taps in Fathi's tests included a portion of the core of the jet as well as some on the outer edge of the jet area. The outer edge of the jet may have produced lower impact pressures. Fathi only presented one pressure value for a certain nozzle diameter, flow rate, and fall height rather than pressures for each of the 17 taps. It was assumed that pressures recorded from the 17 taps were averaged to produce one value of pressure for the jet. When the pressures of all taps were averaged, a lower mean pressure would have resulted if taps on the outer edge of the jet recorded lower pressures than the tap at the center of the jet.

Calculated Impact Force

The impact force of a falling jet against a solid boundary are shown in Figure 13. They were calculated using equations of momentum as shown in Equation 1. The impact velocity of the jet was calculated using Equation 3, which relates acceleration due to gravity, fall height and initial velocity to the impact velocity. The forces against the solid boundary in the CFD model were also recorded for comparison to the calculated values.

The CFD model incorporated any forces on the test platform including forces from the momentum of the falling jet and the weight of the water on the test platform spraying parallel to the platform. The weight of the water was calculated and added to the force calculated due to the momentum of the falling jet to give a more accurate comparison to the forces monitored in the CFD model. The water depth of the spray of water used to calculate the weight of water on the platform was 0.008". This depth is not a true representation of reality. It is only an estimate. The force on the test platform from the CFD model and calculations were plotted together against fall height. The initial velocity was approximately 5 fps in the CFD model and calculations. The

forces from the CFD model and calculations are shown along with the arithmetic difference between the two in Figure 35.

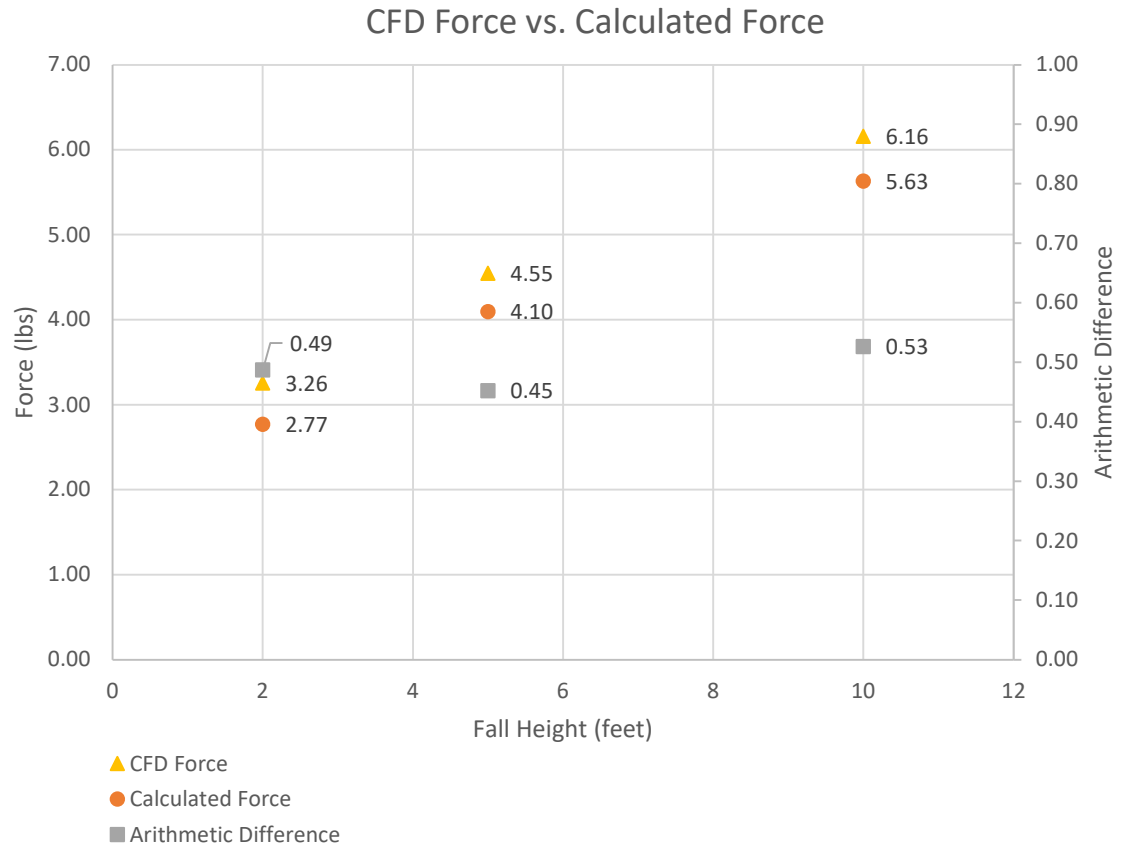


Figure 35 – Force on test platform in CFD model and calculations plotted against fall height.

The calculated forces may not be comprehensive of all forces acting on the testing platform.

There may be other minor forces on the platform, but the major forces from the momentum of the falling jet and weight of the water are included.

Computational Fluid Dynamics Simulation

The greatest difference between the CFD simulation data and laboratory data from the pressure transmitter at approximately 5 fps was 7.2% as shown in Table 2.

Table 2 – Mean pressure (psi) from laboratory tests and CFD at 4.76 fps and 2-ft fall height.

	Fall Height (ft)		
	2	5	10
Pressure Transmitter	0.99	2.05	4.16
CFD	0.92	2.13	3.86
Percent Difference	-7.1%	3.9%	-7.2%

There are no noticeable trends in the difference between CFD and laboratory testing as fall height increased. Further simulations modeling higher flow rates could add beneficial insight into the work of the current study. It appears that the numerical model produced results that closely match the laboratory data.

Repeat Tests

Most of the tests conducted were repeated to give greater confidence in the results. Some of the test configurations were repeated a third time to have at least two data points that produced the same approximate values. It was important to understand the repeatable nature of the pressure measurements in a laboratory setting.

Potential Sources of Error in Laboratory Tests

The test duration and collection frequency were important factors to consider when collecting pressure data for the transducer and the pressure transmitter. A longer test or higher frequency would increase the number of data points collected. This gives more samples from a statistical point of view. The frequency is the number of pressures recorded per second. Most of the tests collected data at 200 Hz for a duration of approximately one minute. Tests were conducted at various frequencies and durations to determine possible effects on the results. As velocity increased, the difference between one data point to an adjacent data point increased. This may signify “gaps” in the data recorded. A higher collection frequency could’ve captured a greater amount of the fluctuation. After establishing repeatability in the data points collected, the tests at 200 Hz for approximately one minute were sufficient for the purposes of this study. Future studies may benefit from conducting tests at higher frequencies or for longer test durations.

Other Variables

The temperature of the water during testing varied between 33.5 °F and 40.3 °F. When the force at impact was calculated using equations of momentum, 32.2 °F and 40 °F were used to determine the density of water. This range of temperatures only produced a percent difference in force at impact on the order of magnitude of 10^{-14} . The different temperatures for various testing were assumed to have an insignificant impact on the resulting impact pressure.

The barometric pressure was recorded for the various tests conducted. The pressure transmitter recorded absolute pressure. The barometric pressure was not used to adjust any resulting data, rather as a check for the data capture with no water running. During some of the final days of testing, the barometric pressure was the lowest for any testing. The zero capture from the pressure transmitter was also noticeably lower on those days. This provided a check for the proper function of the pressure transmitter.

CONCLUSIONS

Previous research provided insight on the physical characteristics of a falling jet. This study provided a simple array of the pressures recorded or calculated using the various instrumentation and methods available. A flush mount transducer, pressure transmitter and piezometer were centered under a falling jet to record pressure. Test configurations included three different fall heights and up to four flow rates. A numerical model using CFD was also built to simulate a few of the same test configurations.

The following are conclusions based on the results and observations discussed in this study:

1. The piezometer, pressure transmitter, and flush mounted transducer will produce similar results at fall heights from 2-5 feet when measuring a falling jet with a circular cross-section at the impact point against a solid boundary. These instruments also produce similar results at a fall height of 10 feet where the jet has a circular cross section, but the pressures obtained from these instruments vary more than at the 2-foot and 5-foot fall heights.
2. It appears that as fall height increases, it has a stronger influence on the impact pressure, and the velocity of the jet has a reduced influence on the impact pressure. As the fall height increased for laboratory tests, the range of pressures recorded for all methods of physical measurement decreased. Further research and testing at fall heights higher than the ones presented here would be helpful to see if the range of pressures continue to decrease with increased fall height.

3. The jet impact diameter is more influenced by the initial jet velocity more than the fall height. The increased velocity, and therefore increased turbulence, may entrain more air and cause the jet to increase in diameter. This rationale is supported by the increased air content for higher velocities as shown in Figure 32.
4. It appears that a flush mounted transducer, pressure transmitter, or piezometer are sufficient instruments for fall heights of 5-feet or less and fall heights of 10-feet when the initial jet velocity is approximately 14 fps or less. The pressures recorded with these three instruments seem to produce very similar results for the 2-foot and 5-foot fall heights and 10-foot fall heights at initial jet velocities of approximately 14 fps or less.
5. When the fall height is 10-feet and the jet initial velocity is approximately 19 fps or greater, a wider range of values may be captured with a flush mounted transducer under the jet compared to the other two instruments. This could be from the turbulence caused by the magnitude of the initial velocity. It is possible that turbulence in the jet develops as the jet falls. With an increased fall height, more turbulence is being developed in the jet. This may signify the capability of the flush mount transducer to record the pressure and lack of pressure from increased air content better than the pressure transmitter and the piezometer.
 - a. The highest values recorded by the flush mounted transducer are found in the FT (3) test series. The values in this series at initial velocities of approximately 19 fps and 22 fps matched the piezometer and pressure transmitter values within about 0.25 psi. The second series, FT (2), is lower than FT (3) at approximately 22 fps by about 0.5 psi. A longer test or higher frequency may be needed to obtain a true average of the pressure using a flush mounted transducer.
 - b. The pressure that must travel through the column of water in the piezometer and pressure transmitter may dampen the pressure signal. This would make it difficult to record some of the data points when the pressure is fluctuating rapidly.

- c. The flush mounted transducer is a more direct method for measuring the fluctuations in a falling jet versus the pressure transmitter and the piezometer.
6. The pressure recorded at different fall heights appears to converge within each mode of physical measurement as shown in Figures 8-10. As velocity increases, it may have a greater influence on the impact pressure than the fall height. Once a certain initial velocity is reached, a change in fall height may not cause a significant change in impact pressure. Further research and testing at flow rates higher than the ones presented here would be helpful to see if the pressures at the three fall heights continue to converge.
7. The presence of air in a falling jet seems to play a key role in the differences of pressures collected with the different laboratory fall heights and flow rates.
8. It is important to bleed the plastic tubing used for piezometers and pressure transmitters very carefully to avoid the presence of air in the tubing. Failing to do so may result in inconsistent pressure readings.
9. Similar results can be obtained from a CFD model and calculations to find the force at the impact point of a falling jet when the jet has an initial velocity of approximately 5 fps and fall heights between 2 and 10 feet. It is important to include the weight of the water on the test platform along with the force from momentum in calculations.
10. CFD simulations are an acceptable method of predicting pressure at the impact point of a falling jet for fall heights between 2 and 10 feet when the initial jet velocity is approximately 5 fps. The simulated pressures may result in very similar results compared to a flush mounted transducer, pressure transmitter under a column of water, and piezometer.

This comparison of various methods of measuring pressure at the impact point of a falling jet is a valuable tool for researchers and practicing engineers when testing physical models in a

laboratory setting. It provides a benchmark for the various options available to determine the pressure under a falling jet at the point of impact. Understanding the differences and similarities between the different methods can guide an engineer when deciding which instrumentation or methods are necessary when constructing and testing a physical model in a laboratory setting.

REFERENCES

- Beltaos, S., and Rajaratnam, N. (1973). "PLANE TURBULENT IMPINGING JETS." *Journal of Hydraulic Research*, 11(1), 29-59.
- Bollaert, E., Manso, P., and Schleiss, A. J. (2004). "Dynamic pressure fluctuations at real-life plunge pool bottoms." *Proc. Int. Conf. Hydraulics of Dams and River Structures*, 117-124.
- Bollaert, E., and Schleiss, A. (2002). "Transient water pressures in joints and formation of rock scour due to high-velocity jet impact."
- Christodoulides, P., and Dias, F. (2010). "Impact of a falling jet." *J.Fluid Mech.*, 657 22-35.
- Ervine, D. A., Falvey, H. T., and Withers, W. (1997). "Pressure fluctuations on plunge pool floors." *Journal of Hydraulic Research*, 35(2), 257-279.
- Fathi-Moghadam, M., Salemnia, A., and Kiani, S. (2019). "Core impact force of vertical water jets on smooth and rough surfaces." *Sci*, 26(2), 690-698.
- Lewis, T. M., Abt, S. R., Wittler, F. R., and Annandale, G. W. (1999). "Predicting Impact Velocities of Developed Jets." *Water Int.*, 24(3), 255-265.
- Manso, P. A., Bollaert, E. F. R., and Schleiss, A. J. (2007). "Impact pressures of turbulent high-velocity jets plunging in pools with flat bottom." *Exp.Fluids*, 42(1), 49-60.
- Nazeer Ahmed. (1987). *Fluid Mechanics*. Engineering Press, Inc., United States of America.
- Puertas, J., and Dolz, J. (2005). "Plunge Pool Pressures Due to a Falling Rectangular Jet." *J.Hydraul.Eng.*, 131(5), 404-407.

APPENDICES

APPENDIX A - CALIBRATION OF MAGNETIC FLOW METER

Table A-1– Utah Water Research Laboratory flow meter calibration data for 6-inch meter.

Manufacturer:	Siemens	Nominal Pipe Dia. =	6-inch			
Calibration Date:	5/13/2022	Pipe Diameter (in.) =	6.000			
Calibration Location:	6-inch line	Pipe Area (ft ²) =	0.20			
		Water Temp. (F) =	45.5			
Meter Serial Number:	112965	Unit Weight (lb/ft ³) =	62.42			
Transmitter S/N:		Kin. Visc. (ft ² /s) =	1.51E-05			
<u>Pipe Setup</u>	Straight Pipe Test					
Upstream:	6-inch standard steel					
Downstream:	6-inch standard steel					
Calibration Performed by:	M. Cannon					
Calibration Witnessed by:	0					
Run No.	UWRL Flow, Qa (gpm)	Indicated Flow, Qi (gpm)	Pipe Velocity (ft/s)	Qi/Qa	Dev. from mean Qi/Qa (%)	Dev. from Qa (%)
1	254.3	254.45	2.89	1.0006	-0.09%	0.065%
2	982.9	985.00	11.15	1.0021	0.06%	0.210%
3	1995.4	1999.00	22.64	1.0018	0.03%	0.183%
			Average=	1.0015		

APPENDIX B - DRAWINGS OF LABORATORY TEST SETUP

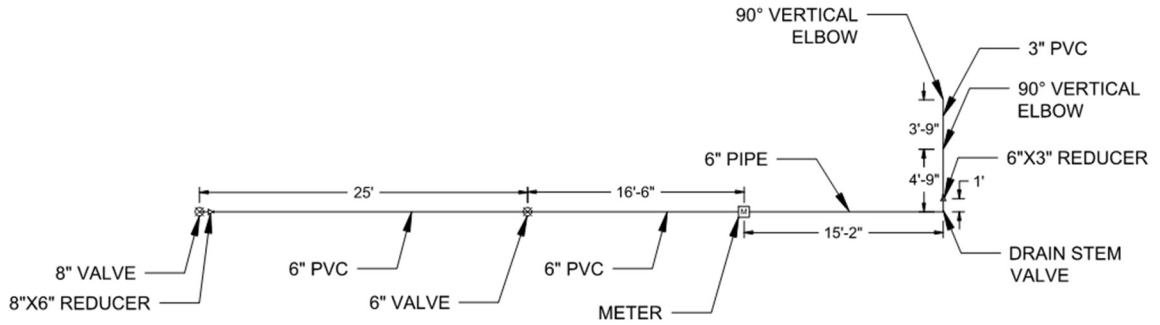


Figure B-1 – Plan view of laboratory testing setup.

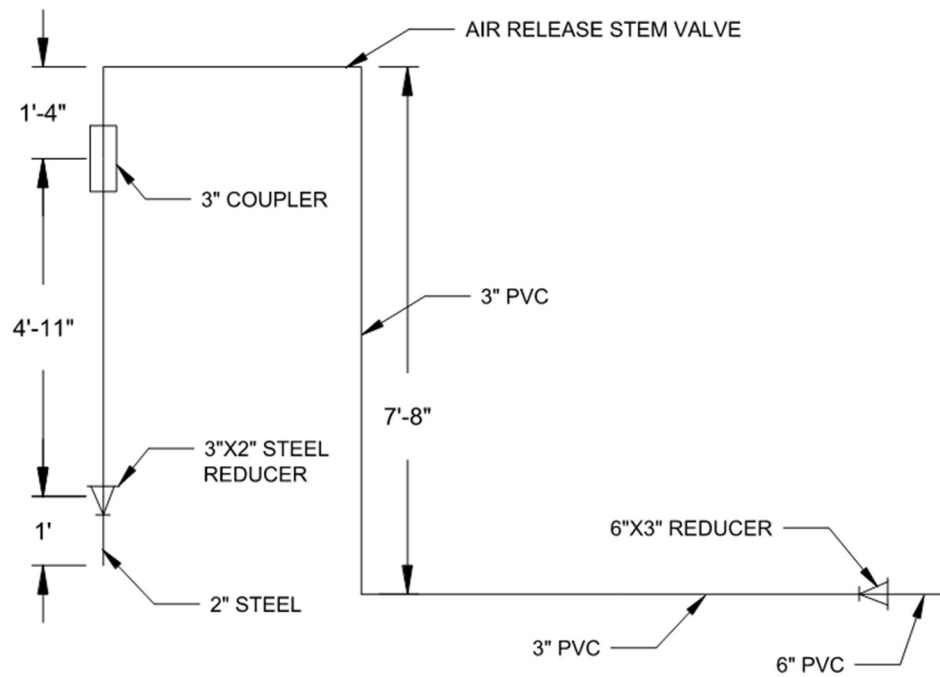


Figure B-2 – Side view of vertical section of laboratory test setup.

APPENDIX C - TABULAR PRESSURES UNDER A FALLING JET

Table C-1 – Pressure recorded under jet for the 1st run at a 2-foot fall height.

Instrument Type	Actual Frequency (Hz)	Initial Velocity (fps)	Fall Height (ft)		Mean (psi)	Standard Deviation (psi)
			Max (psi)	Min (psi)		
			2			
FT	188.6	4.58	1.01	0.41	0.88	0.04
FT	581.3	14.13	1.53	1.07	1.33	0.06
FT	783.3	19.03	4.12	2.81	3.55	0.12
T	196.8	4.78	0.96	0.76	0.89	0.02
T	586.5	14.25	1.44	1.23	1.34	0.04
T	779.9	18.95	2.85	2.46	2.71	0.05
P	190.2	4.62	0.85	0.80	0.83	-
P	590.9	14.36	1.34	1.23	1.31	-
P	781.6	18.99	2.72	2.68	2.70	-

Table C-2 – Pressure recorded under jet for the 1st run at a 5-foot fall height.

Instrument Type	Actual Frequency (Hz)	Initial Velocity (fps)	Fall Height (ft)		Mean (psi)	Standard Deviation (psi)
			Max (psi)	Min (psi)		
			5			
FT	193.6	4.70	2.40	0.95	2.04	0.12
FT	588.6	14.30	4.84	1.91	3.40	0.25
FT	788.0	19.15	5.70	1.29	4.41	0.42
T	186.5	4.53	2.59	1.23	2.11	0.09
T	587.1	14.27	3.64	3.16	3.45	0.06
T	789.2	19.18	4.93	4.03	4.52	0.16
P	191.3	4.65	2.07	1.97	2.04	-
P	590.9	14.36	3.43	3.37	3.41	-
P	787.4	19.13	4.44	4.33	4.41	-

Table C-3 – Pressure recorded under jet for the 1st run at a 10-foot fall height.

			Fall Height (ft) 10			
Instrument Type	Actual Frequency (Hz)	Initial Velocity (fps)	Max (psi)	Min (psi)	Mean (psi)	Standard Deviation (psi)
T	197.2	4.79	4.57	3.80	4.23	0.11
T	583.7	14.18	6.91	1.34	4.96	0.49
T	780.6	18.97	9.43	1.27	5.38	0.89
P	191.8	4.66	4.24	4.12	4.17	-
P	587.7	14.28	5.22	4.78	5.07	-
P	780.1	18.96	5.58	5.00	5.36	-

Table C-4 – Pressure recorded under jet for the 2nd run at a 2-foot fall height.

			Fall Height (ft) 2			
Instrument Type	Actual Frequency (Hz)	Initial Velocity (fps)	Max (psi)	Min (psi)	Mean (psi)	Standard Deviation (psi)
FT	194.3	4.72	1.04	0.85	0.97	0.01
FT	579.0	14.07	1.61	0.90	1.26	0.09
FT	785.2	19.08	4.02	2.74	3.55	0.13
FT	900.2	21.88	5.03	3.30	4.41	0.17
T	198.1	4.81	1.03	0.93	0.99	0.01
T	781.8	19.00	3.96	3.04	3.56	0.11
T	901.5	21.91	5.09	3.70	4.45	0.16
P	202.7	4.93	1.04	1.03	1.03	-
P	597.6	14.52	1.41	1.26	1.35	-
P	782.0	19.00	3.52	3.48	3.50	-
P	900.2	21.88	4.84	4.41	4.48	-

Table C-5 – Pressure recorded under jet for the 2nd run at a 5-foot fall height.

			Fall Height (ft) 5			
Instrument Type	Actual Frequency (Hz)	Initial Velocity (fps)	Max (psi)	Min (psi)	Mean (psi)	Standard Deviation (psi)
FT	196.6	4.78	2.39	1.73	2.17	0.04
FT	589.3	14.32	5.22	1.46	3.27	0.35
FT	780.7	18.97	5.67	1.34	4.28	0.46
FT	899.6	21.86	6.69	1.52	4.92	0.61
T	192.4	4.68	2.29	1.62	2.05	0.07
T	586.7	14.26	3.54	2.98	3.36	0.06
T	780.6	18.97	4.72	3.36	4.15	0.19
T	901.7	21.91	5.53	3.84	4.79	0.26
P	205.0	4.98	2.30	2.28	2.29	-
P	589.6	14.33	3.50	3.47	3.48	-
P	785.0	19.08	4.46	4.37	4.42	-
P	900.9	21.89	5.06	4.98	5.02	-

Table C-6 – Pressure recorded under jet for the 2nd run at a 10-foot fall height.

			Fall Height (ft) 10			
Instrument Type	Actual Frequency (Hz)	Initial Velocity (fps)	Max (psi)	Min (psi)	Mean (psi)	Standard Deviation (psi)
FT	193.7	4.71	6.36	-0.04	3.88	0.72
FT	591.4	14.37	8.50	-0.44	4.73	1.24
FT	781.0	18.98	8.71	-0.69	4.92	1.61
FT	901.3	21.90	9.25	-0.53	4.95	1.80
T	193.0	4.69	4.42	3.78	4.16	0.10
T	905.5	22.00	8.99	0.01	5.41	1.04
P	194.3	4.72	4.26	4.12	4.19	-
P	585.4	14.23	5.09	4.73	4.95	-
P	766.4	18.62	5.45	4.91	5.16	-
P	881.8	21.43	5.63	4.98	5.45	-

Table C-7 – Pressure recorded under jet for the 3rd run at a 2-foot fall height.

			Fall Height (ft) 2			
Instrument Type	Actual Frequency (Hz)	Initial Velocity (fps)	Max (psi)	Min (psi)	Mean (psi)	Standard Deviation (psi)
T	577.6	14.04	1.52	1.18	1.37	0.05
T	784.7	19.07	4.01	3.12	3.59	0.12
P	784.5	19.06	3.61	3.50	3.56	-

Table C-8 – Pressure recorded under jet for the 3rd run at a 5-foot fall height.

			Fall Height (ft) 5			
Instrument Type	Actual Frequency (Hz)	Initial Velocity (fps)	Max (psi)	Min (psi)	Mean (psi)	Standard Deviation (psi)
FT	202.3	4.92	2.48	1.92	2.24	0.06
T	204.5	4.97	2.28	2.21	2.25	0.01
T	591.3	14.37	3.62	3.18	3.45	0.05
T	785.5	19.09	4.89	3.84	4.42	0.16
T	898.9	21.84	5.79	3.92	5.04	0.25

Table C-9 – Pressure recorded under jet for the 3rd run at a 10-foot fall height.

			Fall Height (ft) 10			
Instrument Type	Actual Frequency (Hz)	Initial Velocity (fps)	Max (psi)	Min (psi)	Mean (psi)	Standard Deviation (psi)
FT	193.4	4.70	5.92	0.28	3.87	0.69
FT	587.6	14.28	8.42	-0.47	4.79	1.19
FT	783.0	19.03	8.82	-0.49	5.38	1.41
FT	899.6	21.86	9.07	-0.26	5.54	1.65
T	583.8	14.19	8.25	0.20	4.89	0.57
T	783.3	19.03	8.24	0.58	5.28	0.89

APPENDIX D - LABORATORY TESTING PHOTOGRAPHS



Figure D-1 – Falling jet at approximately 5 fps and 2-foot fall height.



Figure D-2 – Falling jet approximately 14 fps and 2-foot fall height.



Figure D-3 – Falling jet approximately 19 fps and 2-foot fall height.



Figure D-4 – Falling jet approximately 22 fps and 2-foot fall height.



Figure D-5 – Falling jet at approximately 5 fps and 5-foot fall height.



Figure D-6 – Falling jet at approximately 14 fps and 5-foot fall height.



Figure D-7 – Falling jet at approximately 19 fps and 5-foot fall height.



Figure D-8 – Falling jet at approximately 22 fps and 5-foot fall height.



Figure D-9 – Falling jet at approximately 5 fps and 10-foot fall height (upper section).



Figure D-10 – Falling jet at approximately 5 fps and 10-foot fall height (lower section).



Figure D-11 – Falling jet at approximately 14 fps and 10-foot fall height (upper section).



Figure D-12 – Falling jet at approximately 14 fps and 10-foot fall height (lower section).



Figure D-13 – Falling jet at approximately 19 fps and 10-foot fall height (upper section).



Figure D-14 – Falling jet at approximately 19 fps and 10-foot fall height (lower section).



Figure D-15 – Falling jet at approximately 22 fps and 10-foot fall height (upper section).



Figure D-16 – Falling jet at approximately 22 fps and 10-foot fall height (lower section).